Clim Dyn (2018) 50:4037–4060
DOI 10.1007/s00382-017-3860-1

High-resolution projections of mean and extreme precipitations over China through PRECIS under RCPs

Jinxin Zhu[1] · Gordon Huang[1] · Xiuquan Wang[1] · Guanhui Cheng[1] · Yinghui Wu[1]

Received: 19 December 2016 / Accepted: 12 August 2017 / Published online: 22 August 2017

Abstract The impact of global warming on the characteristics of mean and extreme precipitations over China is investigated by using the Providing REgional Climate Impacts for Studies (PRECIS) model. The PRECIS model was driven by the Hadley Centre Global Environment Model version 2 with Earth System components and coupling (HadGEM2-ES). The results of both models are analyzed in terms of mean precipitation and indices of precipitation extremes (R95p, R99p, SDII, WDF, and CWD) over China at the resolution of 25 km under the Representative Concentration Pathways 4.5 and 8.5 (RCP4.5 and RCP8.5) scenarios for the baseline period (1976–2005) and two future periods (2036–2065 and 2070–2099). With improved resolution, the PRECIS model is able to better represent the fine-scale physical process than HadGEM2-ES. It can provide reliable spatial patterns of precipitation and its related extremes with high correlations to observations. Moreover, there is a notable improvement in temporal patterns simulation through the PRECIS model. The PRECIS model better reproduces the regional annual cycle and frequencies of daily precipitation intensity than its driving GCM. Under RCP4.5 and RCP8.5, both the HadGEM2-ES and the precis project increasing annual precipitation over the entire country for two future periods. Precipitation increase in winter is greater than the increase in summer. The results suggest that increased radiative forcing from RCP4.5 to RCP8.5 would further intensify the magnitude of projected precipitation changes by both PRECIS and HadGEM2-ES. For example, some parts of south China with decreased precipitation under RCP4.5 would expect even less precipitation under RCP8.5; regions (northwest, northcentral and northeast China) with increased precipitation under RCP4.5 would expect more precipitation under RCP8.5. Apart from the projected increase in annual total precipitation, the results also suggest that there will be an increase in the days with precipitation higher than 15 mm and a decrease in the days with precipitation less than 5 mm. Under both RCPs, there would be an increasing trend in the magnitude of changes in precipitation extremes indices (R95p, R99p, and SDII) over China, while an opposite trend is projected for CWD and no apparent trend is projected for WDF from 2036–2065 to 2070–2099. Increased extreme precipitation amounts accompanied with decreased frequencies of extreme precipitation suggest that the future daily extreme precipitation intensity is likely to become large in northeast China and south China.

Keywords Precipitation and extremes · Dynamical downscaling · PRECIS · China · RCP4.5 and RCP8.5

1 Introduction

China has various climates due to its large landmass, complex topography and large-scale Asian monsoon driven by the temperature differences between the Asia continent and the Pacific Ocean (Li et al. 2011a, b). The various climates make China sensitive to the effects of climate change mainly in the fields of agriculture, forestry, fishery, ecosystems and water resources. Particularly, extreme precipitation events can cause extensive damages to various systems and undo socioeconomic structures decades in the making. For example, south China suffered from a severe snow storm in early 2008. Heavy snows caused extensive damage, power systems

✉ Gordon Huang
huang@iseis.org

[1] Institute for Energy, Environment and Sustainability Research, University of Regina, Regina, SK S4S 0A2, Canada

failure, crops loss and transportation disruption for almost half the whole territory. The direct economic losses inflicted by the storm were over $20 billion (Zhou et al. 2011). The heaviest rainfall in 60 years hit Beijing on July 21st, 2012. Around 175–200 mm fell over much of the city within 10 h. It caused the estimated $1.5 billion economic losses and 1.9 million people affected by the downpour and flood (Zhou et al. 2013; Zheng et al. 2016). Substantial researches demonstrate that precipitation, particularly extreme precipitation, from climate system is susceptible to the global warming (Karl et al. 1995; Wood et al. 1997; Held and Soden 2006; Seager et al. 2007; Hartmann et al. 2013). Therefore, studying how the global warming may change the precipitation over China in the future has great significance. Climate models play a crucial role in facilitating researchers to study climate systems and climate change (Chen and Sun 2009). General circulation model (GCMs) are widely used to reproducing large-scale climates (Xu and Xu 2012; Sperber et al. 2013; Kitoh et al. 2013; Gong et al. 2014) and projecting response of them to future external forcing with roughly 1–2° spatial resolution (Taylor et al. 2012). With coarse resolutions, GCMs are incapable of representing many processes that drive regional climate variability, especially in terms of reflecting extreme precipitation events (Huang et al. 2013; Bucchignani et al. 2014; Bao et al. 2015). Extreme precipitation takes place on a very small spatial scale which makes GCMs unable to simulate (Wehner et al. 2010; Feng et al. 2011; White et al. 2013). There is some progress in improving the resolution of GCMs in the phase five of the Coupled model intercomparison project (CMIP5) (Taylor et al. 2012; Lee et al. 2014), but their resolution is still too coarse to be applied for down streams at the regional scale. By contrast, Regional Climate Models (RCMs) can represent fine-scale physics processes and dynamically downscale the initial and lateral boundary conditions from GCMs to provide regional information and (Giorgi and Mearns 1991; Giorgi 2006; Christensen et al. 2007; Liang et al. 2008; Giorgi et al. 2009; Colette et al. 2012; Racherla et al. 2012; Hewitson et al. 2014; Ji and Kang 2015). RCMs make high-resolution information available for downstream application and have been widely used to obtain historical climate simulations and future projections over China (Hirakuchi and Giorgi 1995; Gao et al. 2001, 2011, 2012; Yu et al. 2010; Sato and Xue 2013).

Previously, a number of studies have been carried out for simulating climatic changes over China. For example, the Regional Climate Model system (RegCM) was developed to downscale the National Center for Atmospheric Research (NCAR) Community Climate System Model over China (Liu et al. 2013). RegCM produced high spatial pattern correlations with observations for precipitation and surface air temperature, and corrected some wet and cold biases in its driving GCM. The Flexible Global Ocean–Atmosphere–Land System model, grid point version 2 (FGOALS-g2) was also downscaled through RegCM over China (Zou and Zhou 2013). RegCM was able to reproduce the spatial distribution of extreme summer precipitation and projected more intensified changes in extreme precipitation than FGOALS-g2. Most recently, the Beijing Climate Center Climate System Model version 1.1 (BCC-CSM1.1) was adopted to downscaled to simulate climate change through RegCM over China. It is also shown that RegCM improved the climate simulation (Gao et al. 2013). Results from regional climate model COSMO-CLM (CCLM) downscaling the European Centre/Hamburg version 5 (ECHAM5) over East Asia shown that CCLM could reasonably capture the regional climate features, but CCLM simulated a wet bias over some parts of China (Wang et al. 2013). The weather research forecasting (WRF) model driven by the operational seasonal forecast model Climate Forecast System (CFS) was used to downscale the annual and seasonal precipitation over the continental China. WRF was capable of reducing the wet bias of seasonal mean precipitation and improve inter-annual variations over regions (Yuan et al. 2012). The WRF model has the ability to simulate the mean and extreme precipitations over China was also examined through downscaling the Geophysical Fluid Dynamics Laboratory Earth System Model with the Generalized Ocean Layer Dynamics component (GFDL-ESM2G) (Dunne et al. 2012; Bao et al. 2015). WRF successfully eliminated some artificial precipitation maximum areas and provided more reliable spatial distributions of total and extreme precipitation in China. As for the Providing REgional Climate Impacts for Studies (PRECIS) model (Wilson et al. 2015), there are some researches had been done through it for downscaling the Hadley Centre Coupled Model version 3 (HadCM3) over China under Special Report on Emissions Scenarios B2 (SRES B2) scenario (Xu et al. 2006). The regional model's ability to simulate the historical and future climate of China was tested and verified.

Many studies indicate that the CMIP5 multi-model has an improved representation of rainfall compared to the CMIP3 (Sperber et al. 2013; Sun et al. 2015; Yan et al. 2015; Zhang et al. 2015). This is reflected by the more realistic magnitude of rainfall in terms of the skill of simulating pattern correlations with respect to observations. Additionally, for rainfall/convection the CMIP5 models outperforms the CMIP3 models for the time mean, the inter-annual variability of the East Asian monsoon, and inter-seasonal variability.

Previous studies have demonstrated the RCMs are good at adding value to GCMs' simulations over China. However, most of them were in 50 km resolution and based on the results of CMIP3. With the release of CMIP5, most of the studies suggests there will be substantial changes in the precipitation under RCPs compared with SRES scenarios (Vuuren et al. 2011; Taylor et al. 2012; Chen and Frauenfeld

2014). Therefore, it is necessary to investigate how the mean and extreme precipitation over China will response under any representative concentration pathways scenarios.

The aim of this study is to carry out a total of 95 years (2005–2099) transient simulation of precipitation (including total precipitation and extreme precipitation) over China under RCPs at 25 km grid cells. To archive this, the historical simulation of precipitation for both PRECIS and its driving GCM will be validated with the observation dataset regarding spatial and temporal patterns. The future precipitation will be simulated by PRECIS under RCPs and analyzed with respected to changes in the mean precipitation and selected indices of extremes. The paper is organized as follows. Section 2 will describe model details, experimental design, and data. Evaluation of historical simulation in terms of total precipitation and extreme precipitation by the models will be shown in Sect. 3. Future projections under the two RCPs will be presented in Sect. 4. The final section will provide the summary and conclusions.

2 Models, experiment design and data

The regional climate model used in the present study is the PRECIS model version 2.0.0 developed by Met Office Hadley Centre, UK (Jones et al. 2004; Wilson et al. 2015). It is an atmospheric and land surface model of limited area and high resolution which is originally designed to serve both operational forecasting and atmospheric research needs. Dynamical flow, the atmospheric sulfur cycle, clouds and precipitation, radiative processes, the land surface and the deep soil are all described. The PRECIS model has been widely applied in regional simulations (Xu et al. 2006; Feng et al. 2012; Wang et al. 2014, 2015), and its ability in climatological mean and extreme climate simulations over China has been tested and verified (Xu et al. 2009). Moreover, PRECIS exhibits improved performance in simulating the inter-annual variations presented by its driving data (Wang et al. 2016).

Hadley Centre Global Environment Model version 2—Earth Systems (HadGEM2-ES) provides the meteorological forcing at the limits of the PRECIS model's domain as its lateral boundary conditions (LBC) to produce the high-resolution historical simulation and future projection (Collins et al. 2008). Though over 40 models participated in CMIP5, only 11 of these models had the added capability to explicitly represent biogeochemical processes that interact with the physical. climate biogeochemical processes that interact with the physical climate. It means that the global climate models are Earth System Models (ESMs). These 11 ESMs are: BCC_CSM1.1, BNU-ESM, CanESM2, GFDL-ESM2G, GFDL-ESM2M, INM-CM4.0, IPSL-CM5A-MR, MIROC-ESM, MIROC-ESM-CHEM, NorESM1-M and HadGEM2-ES (MACA 2017). Distinctive to others, HadGEM2-ES has the highest resolution among these ESMs incorporated dynamic vegetation (Martin et al. 2011; Jiang et al. 2015). Studies indicate that higher horizontal resolution is associated with the enhanced skill in representing the climate variables in the CMIP5 models (Rupp et al. 2013; Zhang et al. 2013). Plus, there are studies carried out to examine their capacities to simulate the interested variables (i.e. minimum/maximum temperature, precipitation, wind, humidity, solar radiation). Overall, HadGEM2-ES is the best model in most variables especially surface conditions and atmospheric circulation in these studies.

PRECIS computational domain is centered at (34°N, 105°E), and it covers China with 292 × 186 horizontal grid points and a lateral buffer zone of 20 grid points. The spatial resolution is 0.22° × 0.22°. PRECIS runs are integrated continuously during 1969–2005 for the historical simulation and 2006–2099 for the future projections. Future projection simulations are forced with specified concentrations consistent with a medium emission scenario (RCP4.5) and a high emission scenario (RCP8.5). RCP4.5 is a stabilization scenario, with the total radiative forcing of 4.5 W/m^2 until 2100. RCP8.5 is a scenario of comparatively high greenhouse gas emissions with stabilizing near 8.5 W/m^2 (Moss et al. 2010). With these two RCP scenarios, changes in precipitation can be investigated under increasing radiative forcing.

Considering the internal regional features of precipitation in China and based on some previous studies (Li et al. 2011a, b; Luo et al. 2013; Bucchignani et al. 2014; Guo et al. 2017), we divide the contiguous China domain into five sub-regions, namely northwest China, northcentral China, Tibet, northeast China, and south China. As shown in Fig. 1, these sub-regions are typically used in weather and climate related discussions in China because of the climatic similarities within each sub-region. The five sub-regions represent five distinct climate types which are dry, warm, plateau, cold,

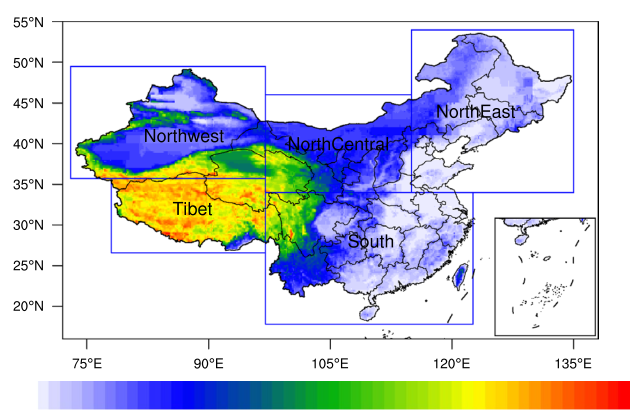

Fig. 1 Model domain, topography (unit: m), and the five sub-regions: Northwest, Northcentral, Northeast, Tibet and South

and wet climate. For each sub-region, we calculate the area-averaged precipitation for the validation and undermentioned differences in total and extreme precipitation changes. Five precipitation indices are used in this study (Table 1). They are described in detail by Frich et al. (2002) and Zou and Zhou (2013), including percentage of wed days exceeding 95 percentile (R95p), percentage of wed days exceeding 99 percentile (R99p), simple daily intensity index (SDII), wet-day frequency (WDF), and consecutive wet days (CWD). To assess the skills of model simulations of the historical climate, observational data are needed as references to compare with the model results. The observed precipitation and temperature (used in examine Clausius–Clapeyron relation) is from APHRODITE's (Asian Precipitation–Highly-Resolved Observational Data Integration Towards Evaluation) gridded daily precipitation and temperature dataset with a spatial resolution of 0.25°×0.25° (Yatagai et al. 2012). The APHRODITE dataset is based on the interpolation from more than 5000 valid stations across Asia and covers a period of more than 50 years. It applies enhancement of quality control algorithm to develop the only Asian precipitation products highly resolved in time and space.

3 Historical simulation of precipitation

Figure 2 shows the spatial distribution of annual, winter and summer mean precipitation over China from HadGEM2-ES, PRECIS, and APHRODITE for the period from 1976 to 2005. Three months' result, namely June, July and August (JJA) in summer, and December, January and February (DJF) in winter are selected to calculating the two-seasonal mean precipitation. APHRODITE shows that annual mean precipitation amounts are relatively low over northwest China, increasing southeastward and reaching the maximum at the southwest of Yunnan-Kweichow Plateau (located in between 22°N and 30°N, 100°E and 111°E) in south China. The mean precipitation for winter and summer also exhibit similar spatial distribution. But the summer precipitation amounts outweigh the winter's due to the nature of monsoon climate in East Asia. Comparing to APHRODITE, HadGEM2-ES simulates the annual mean precipitation in a different spatial pattern, the precipitation amount increasing southward. The simulated precipitation amounts are higher than the observations' over south China and Tibetan Plateau. There is an artificial strong precipitation area simulated by HadGEM2-ES over the west of Tarim Basin in northwest China along the southern edge of the Tibetan Plateau in both seasons. The overestimation of precipitation here is a common occurrence in many other GCMs with coarse resolution (Flato et al. 2013). PRECIS significantly reduces their occurrences and reproduces better spatial patterns of mean precipitation. Furthermore, PRECIS captures the observational maximum precipitation area locating at the southwest of Yunnan-Kweichow Plateau and eliminates the artificial strong precipitation area over the Tarim Basin in both seasons. These results are congruent with previous studies that employed other RCMs such as RegCM and WRF to simulate the historical climate over China (Gao et al. 2008; Zou and Zhou 2013; Bao et al. 2015). It should be noticed that the PRECIS model is not implicitly perfect since the simulated precipitation is overestimated over south China and Tibetan Plateau in winter. Generally, major model biases in simulating present-day climate would be systematically propagated into future climate projections at regional scales (Liang et al. 2008; Xue et al. 2014). A more accurate simulation of present-day climate provides confidence that future projections are more credible (Wang et al. 2016). In this study, we will use the simulations to calculate the percentage changes in precipitation to minimize the effects of the modeling bias on the reliability of future precipitation projections. Future precipitation projections will be developed by applying the projected changes to the observed precipitation for the current climate of China. In this sense, the developed precipitation projections in this study will be bias-corrected and thus can provide helpful information for assessing the potential effects of climate change in the context of China. Besides, there is a study showing that bias correction

Table 1 Definitions of extreme precipitation indices used in this study

Labels	Name	Index definition	Units
R95p	Percentage of wed days exceeding 95 percentiles	The percentage of wet days (define a wet day as having precipitation ≥1 mm/day) with daily precipitation exceeding the 95th percentile of the daily precipitation at wet days	%
R99p	Percentage of wed days exceeding 99 percentiles	The percentage of wet days where the daily precipitation amount is over the 99th percentile of the daily precipitation amount at wet days	%
SDII	Simple daily intensity index	The daily mean intensity of a time series of daily precipitation amounts at wet days	mm/day
WDF	Wet-day frequency	The percentage of days in baseline period which are wet days	%
CWD	Consecutive wet days	The largest numbers of consecutive wet days of a time series of daily precipitation	day

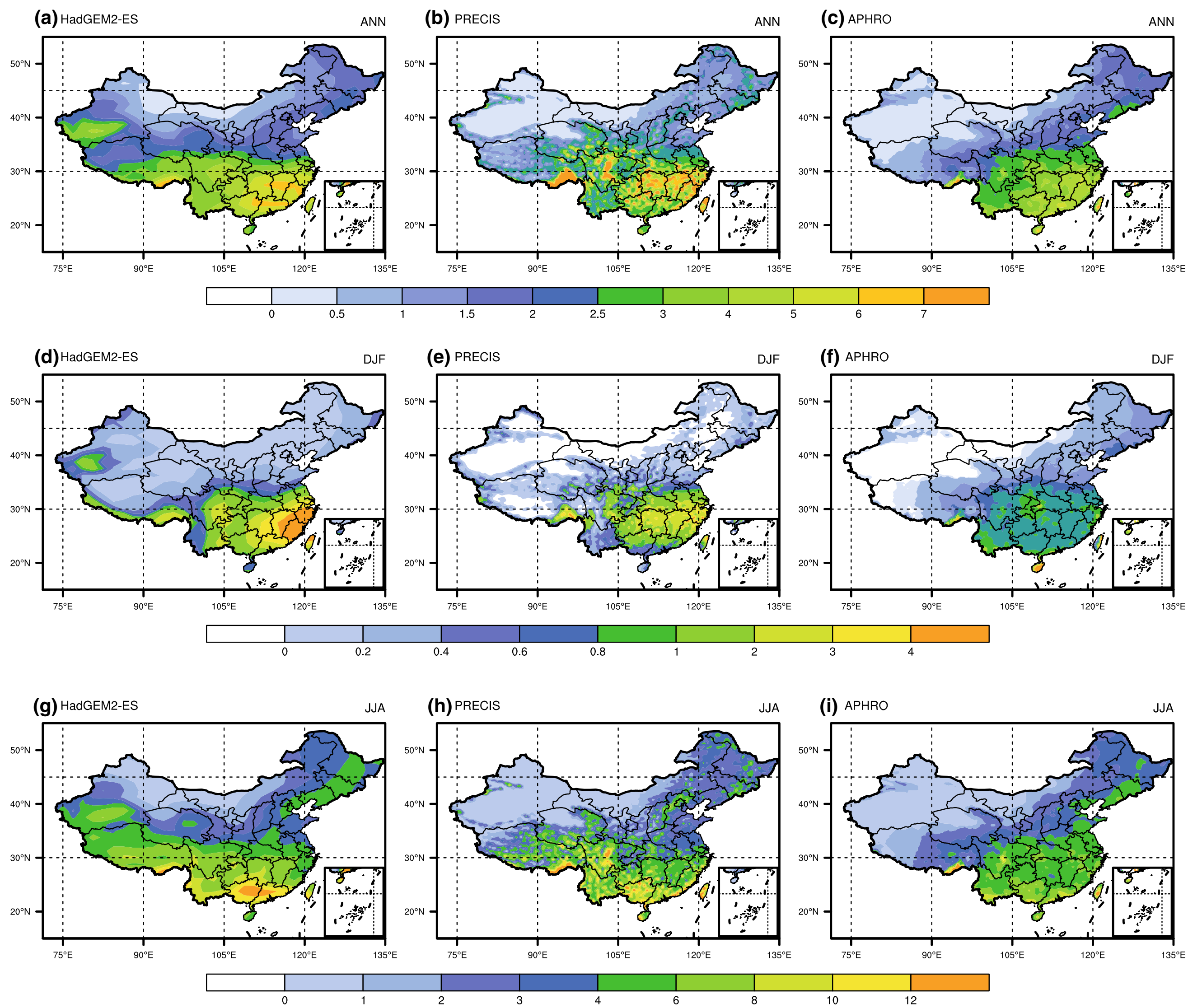

Fig. 2 Spatial distributions of precipitation (unit: mm/day) for 1976–2005 over China from HadGEM2-ES (**a, d, g**), PRECIS (**b, e, h**), and observations (APHRO referred as APHRODITE) (**c, f, i**)

methods impaired the GCM advantages by altering spatiotemporal field consistency and relations among variables, they largely neglected the feedback mechanisms (Ehret et al. 2012). Thus, the validity of correcting the model bias using bias correction methods still remains to be verified. But it is indubitable that PRECIS more reasonably captures spatial patterns than HadGEM2-ES does in both seasons.

To gauge the skills of HadGEM2-ES and PRECIS in reproducing the annual, summer and winter mean precipitation, the Taylor Diagram is introduced to summarize how closely the patterns from two models' results match the observation (Taylor 2001). It exhibits the correlation coefficient (COR), standard deviation (SD), and root-mean-square error (RMSE) between simulated patterns and the observational pattern in a graphical way. The simulated pattern with the right amplitude of its variations (represented by SD), high correlation, and low RMSE agrees well with the observation. On the plot, the pattern will have a closer distance to the reference point marked "OBS" on the x-axis. Figure 3 shows the relative merits of HadGEM2-ES and PRECIS with respect to reproducing the spatial patterns of annual, summer and winter mean precipitation for China and five sub-regions. In comparison with HadGEM2-ES, all the annual and two seasons' results from PRECIS have CORs between 0.6 and 0.9, and SDs between 1 and 1.5 for China, which indicates that PRECIS has reasonable performance in simulating the spatial distribution of precipitation. Overall, PRECIS has a relatively high skill of reproducing the spatial distribution of mean precipitation in both seasons over China. As for the five sub-regions, PRECIS still performs

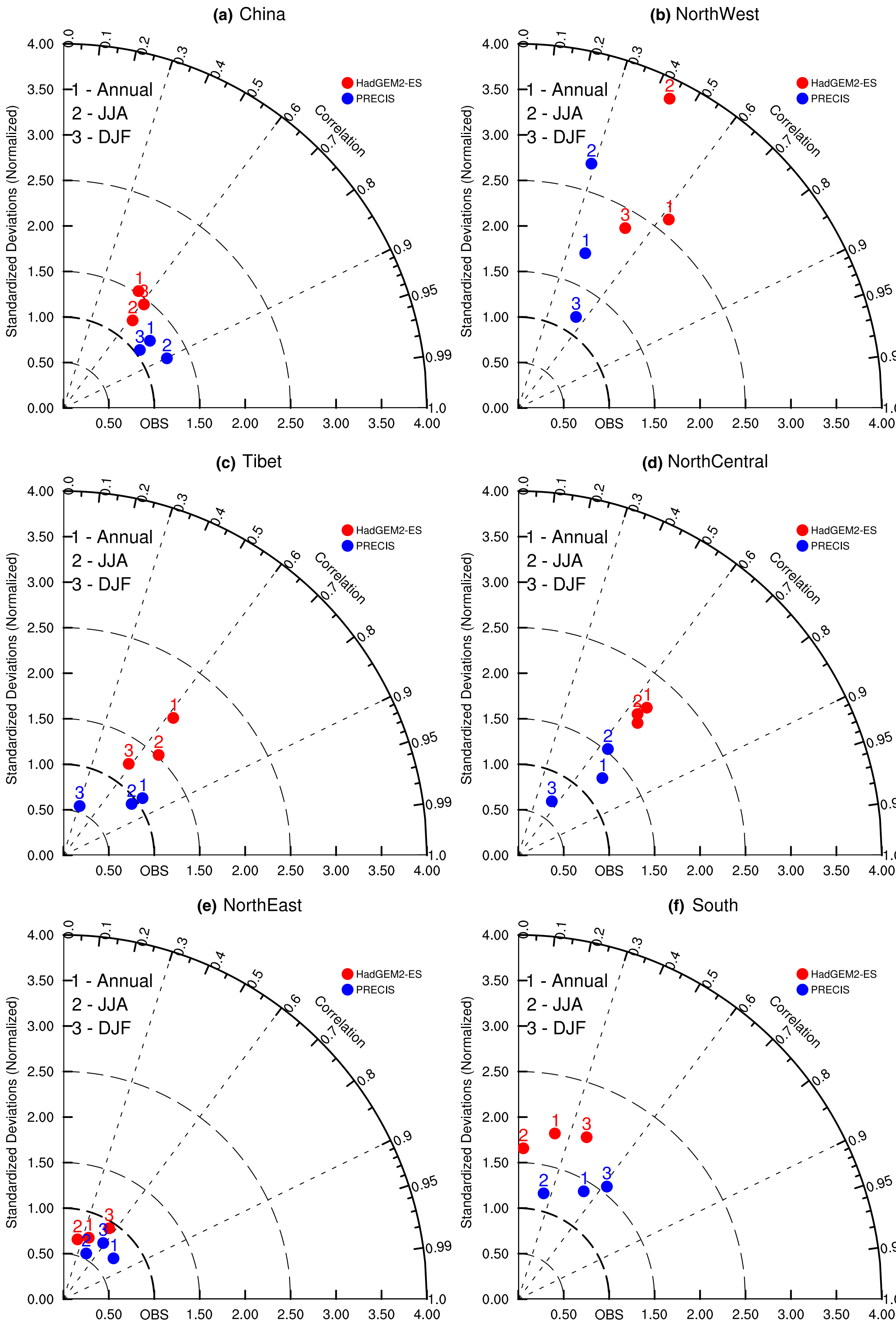

Fig. 3 Comparison of model simulations of precipitation during 1976–2005 over China and five sub-regions in Taylor diagrams

better than HadGEM2-ES in simulating annual, summer and winter precipitation, but PRECIS, itself, shows an inconsistent performance level at the different sub-region. Results of PRECIS over northwest China have the lowest CORs and highest RMSEs compared with the results of other four regions. The poor performance of PRECIS could be caused by its driving GCM since HadGEM2-ES, here, simulates the highest RMSE and SD among all five sub-regions. Simulated patterns of PRECIS over Tibetan Plateau agrees best with the observation as they have the lowest RMSEs and highest CORs for both seasons. However, the relatively high skill of PRECIS in simulating spatial patterns is not necessarily related to the inputs of the driving GCM because the performance of HadGEM2-ES over Tibetan Plateau is not the best. The high skill of PRECIS may result from the model's inherent capacity of simulating the precipitation in high altitude areas. Overall, it is evident that PRECIS outperforms HadGEM2-ES in respect of simulating the spatial distributions of annual, summer, and winter precipitation for China and five sub-regions.

Figure 4 demonstrates the annual cycles of precipitation estimated from two models' outputs and the observational data for China and five sub-regions. For China, the curve of PRECIS well matches the annual cycle of APHRODITE. It is noteworthy that the maximum value of the curve equals to the value of observational curve. Though HadGEM2-ES does capture the trends of the observed annual cycle, it holistically overestimates the amount ranging from 0.5 to 1.9 mm/day. For northwest China, the contrast between two models' results is more obvious than that for the entire

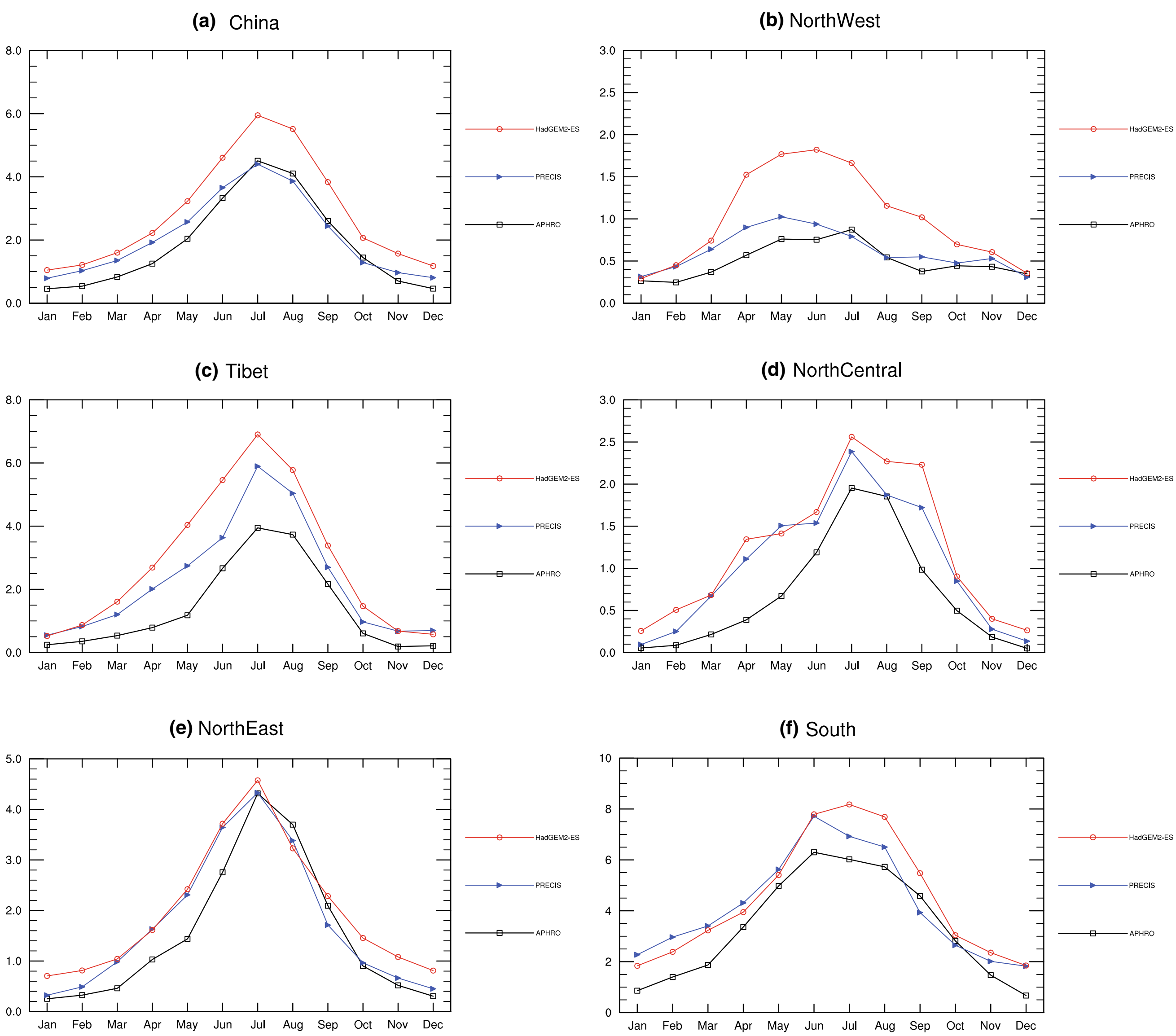

Fig. 4 Annual cycle of precipitation (unit: mm/day) over China and the five sub-regions during 1976–2005

country. The annual cycle for PRECIS agrees with the observational cycle, while the cycle for HadGEM2-ES towers above the observation for all months with the maximum difference up to 250% of the reference value. However, PRECIS overestimates the precipitation amounts before July, and both models simulate an earlier wet season. As for Tibet, both models over simulate precipitation amounts for the full cycle, but values of PRECIS are closer to the observation than those of HadGEM2-ES. For northcentral China, two models' results exhibit overestimations in all seasons and especially in spring and autumn. Nonetheless, both PRECIS and HadGEM2-ES do capture the wettest month, July. For northeast China, the annual cycles of HadGEM2-ES and PRECIS generally stick together from March to August and reach the maximum at July which is the observed wettest month. But the results of PRECIS match the observation better than HadGEM2-ES for the months before March and after September. For south China, HadGEM2-ES simulate July as the wettest month in the annual cycle, whereas the month with maximum precipitation is June in the PRECIS simulation and the observation. Based on the results above, PRECIS is more reliable than HadGEM2-ES to represent the annual cycles for China and all five sub-regions.

Figure 5 shows the histograms of the frequency distribution of the daily precipitation intensity of PRECIS, HadGEM2-ES, and APHRODITE for the baseline period over five sub-regions. For each chart, it takes the daily precipitation data of every grid cell in the selected region into account for the analysis. Each column represents the percentage of days that all grids' precipitation amounts in a subregion falling into a range (0–5, 5–10, 10–15, 15–20, 20–30 and >30) for 30 years. Compared with the observation, both simulations tend to underestimate the frequencies of daily precipitation intensities below 5 mm/day and overestimate the frequencies of daily precipitation intensities between 5 mm/day and 30 mm/day for five sub-regions. However, the PRECIS model performs better than HadGEM2-ES as its results are more accordant with APHRODITE data. Moreover, the observed shifting of the daily precipitation amount distribution toward heavy precipitation is in agreement with a recent published study (Ma et al. 2017). Ma et al. provide evidence that the observed shift from weak precipitation to intense precipitation is primarily due to the contribution of increased radiative forcing, with anthropogenic aerosols forcing offsetting some of the effects of the increased radiative forcing during the second half of the twentieth century. Anthropogenic aerosols from air pollution can affect precipitation via aerosol-radiation interaction (ARI) and aerosol-cloud interaction (ACI) effects (Li et al. 2017). While the ARI effect is included in most of CMIP5 models, only a very small number of models fully or partially include the ACI effect, which implies that current climate models do not have all the capacities needed to fully represent the multiple aerosol effects on precipitation. The aerosol group from Met Office develops the aerosols emission, transport, and deposition schemes, and the interaction of aerosols with radiation and clouds within the PRECIS model to make the simulated results more consistent with observations (Mulcahy et al. 2014).

In Fig. 6, simulated indices of precipitation extremes (R95p, R99p, SDII, WDF, and CWD) from HadGEM2-ES and PRECIS are validated with indices derived from the observation for the baseline period. R95p is defined as the percentage of wet days (define a wet day as having precipitation ≥1 mm/day) with daily precipitation exceeding the 95th percentile of the daily precipitation at wet days for the baseline period. The spatial patterns of R95p (Fig. 6a–c) is well simulated by PRECIS. High values of the wet days with extreme precipitation over the east part of south China and southwest of Yunnan-Kweichow Plateau are well captured. Low values of the index over northwest China, Tibet, and northcentral China are also very well produced. HadGEM2-ES tends to greatly overestimate the high values over southeast China and low values over northwest China and Tibet. HadGEM2-ES fails to capture the maximum values of the index over the southwest of Yunnan-Kweichow Plateau. As for R99p (Fig. 6d–f), it is defined as the percentage of wet days where the daily precipitation amount is over the 99th percentile of the daily precipitation amount at wet days for the given reference period. Both models have a similar spatial distribution with observations', but they slightly overestimate values of the index over southeast China and Tibetan Plateau, and underestimate the values over the southwest of Yunnan-Kweichow Plateau. PRECIS better captures the low values of R99p over northeast China than HadGEM2-ES does. The Simple Daily Intensity Index (SDII) is defined as the daily mean intensity of a time series of daily precipitation amounts at wet days. As shown in Fig. 6g–i, there is good agreement between the PRECIS simulating SDII and the observed SDII over China. However, SDII is underestimated in the model over northwest China and south China. Despite the simulation over Tibet, HadGEM2-ES largely underestimate SDII all over China. The Wet Day Frequency (WDF) is defined as the percentage of days in baseline period which are wet days. The simulated WDF and observed WDF are shown in Fig. 6j–l. High frequencies of wet days over the southwest of Yunnan-Kweichow Plateau and low frequencies over northwest China and northcentral China are well simulated by PRECIS. HadGEM2-ES, whereas, highly overestimate the index for the Sichuan Basin with the maximum value being 70%. Figure 6m–o show the spatial distribution of the Consecutive Wet Days (CWD) per baseline period over China. The index presents the largest numbers of consecutive wet days of a time series of daily precipitation. The CWD is more in south China and Tibet, and less in northwest China for both models. These spatial

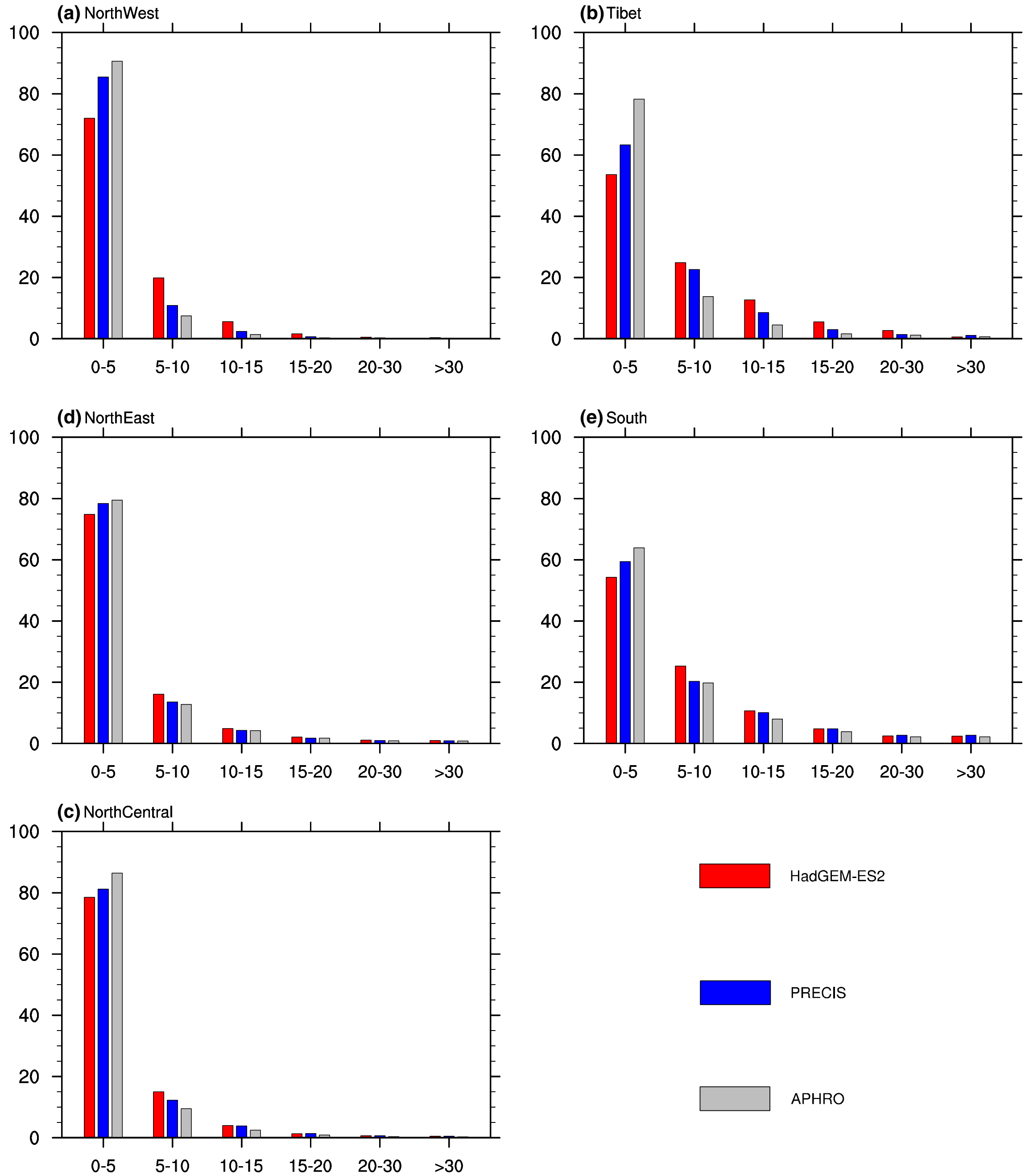

Fig. 5 Frequencies (unit of axis y: %) of daily precipitation intensities (unit of axis x: mm/day) of model simulations and observations over the five sub-regions for 1976–2005

patterns are well captured by PRECIS. The index is largely overestimated by HadGEM2-ES over China except for the two sub-regions, northeast China and northcentral China. Therefore, it is unequivocal that PRECIS better depicts spatial distributions of extreme precipitation than HadGEM2-ES simulation does for China.

In Fig. 7, regional statistics are shown for indices of precipitation extremes derived from two models and the observation over five sub-regions. Overall, results of PRECIS are more consistent with the observation data than results of HadGEM2-ES are. PRECIS gives more reliable and reasonable regional averages of indices of precipitation extremes for China. In northwest China, both models tend to overestimate R95p, R99p, WDF, and CWD and underestimate SDII. However, HadGEM2-ES simulates much higher values for R95p, R99p, WDF, and CWD and lower value for SDII in comparison with APHRODITE. In Tibet and northcentral China, both models produce higher

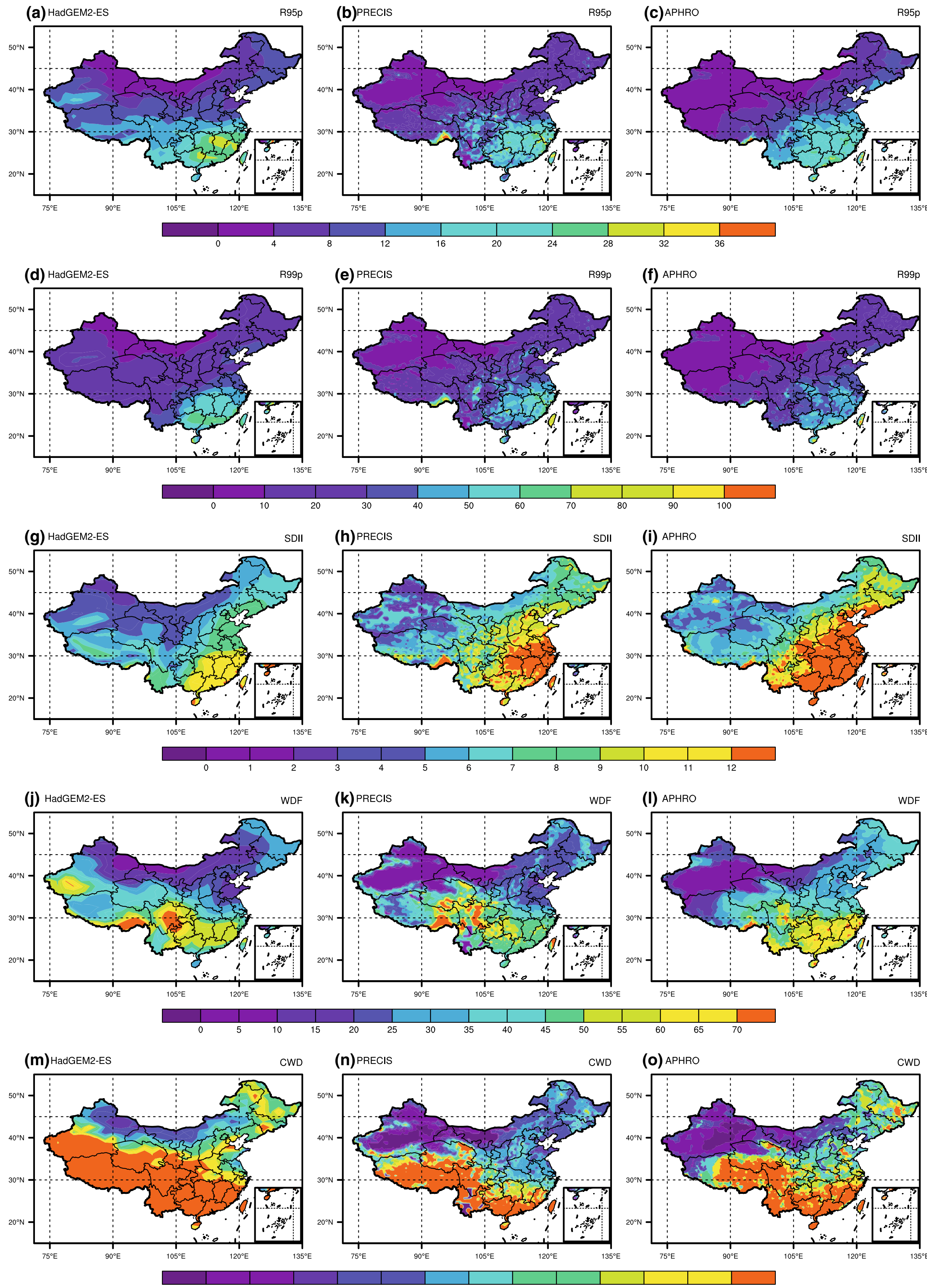

Fig. 6 Spatial distributions of indices of annual mean precipitation extreme (R95p, unit: %; R99p, unit: %; SDII, unit: mm/day; WDF, unit: %; and CWD, unit: days) over China for HadGEM2-ES, PRECIS, and observations from 1976 to 2005

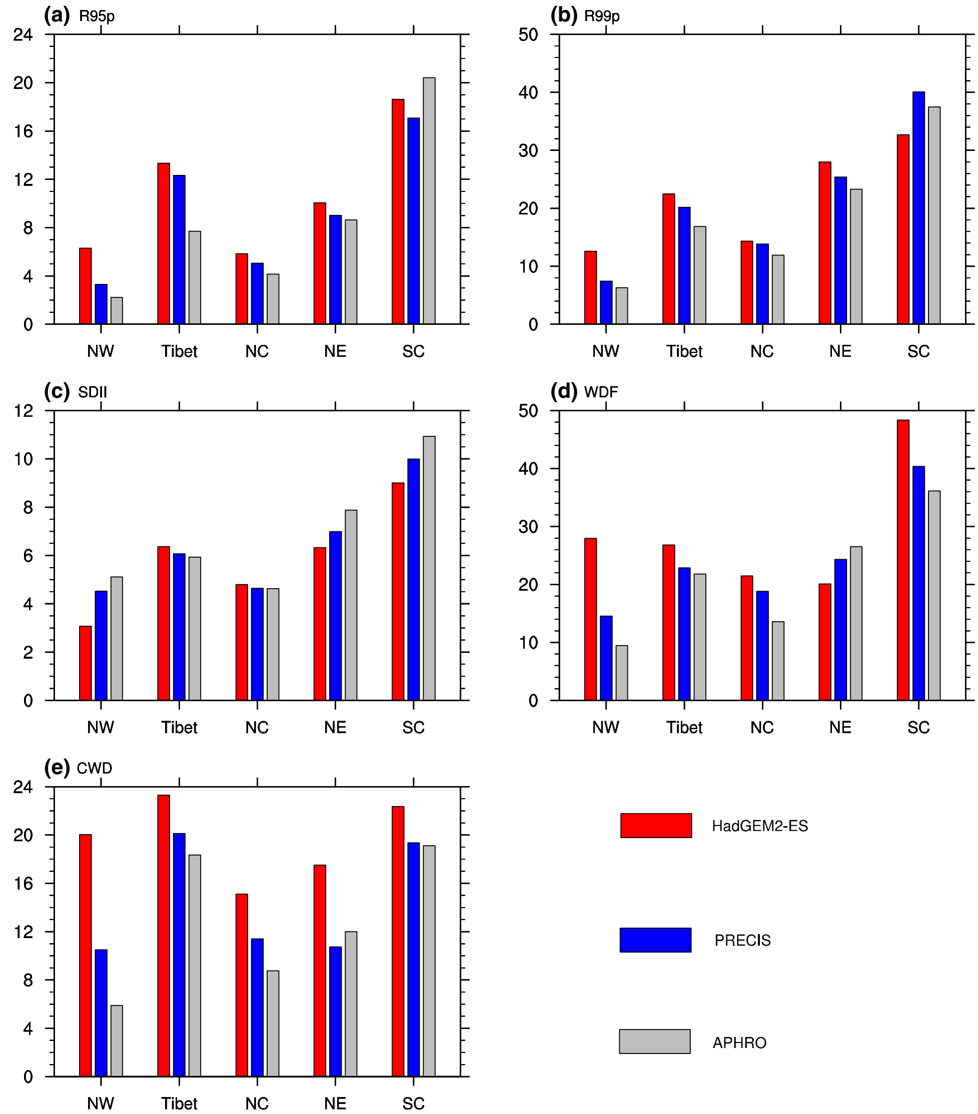

Fig. 7 Regional averages for indices of annual mean precipitation extreme (R95p, unit: %; R99p, unit: %; SDII, unit: mm/day; WDF, unit: %; and CWD, unit: days) for HadGEM2-ES, PRECIS, and observations

values of all five indices than the observation. In northeast China, HadGEM2-ES overestimates the averages of R95p, R99p, and CWD and underestimates the averages of SDII and WDF. PRECIS simulating indices are consistent with results of HadGEM2-ES excepting on CWD which is underestimated by PRECIS. In south China, HadGEM2-ES underestimates the averages of R95p, R99p, and SDII and overestimates the averages of WDF and CWD. PRECIS is only consistent with HadGEM2-ES for R95p, SDII, and WDF. For R99p and CWD, PRECIS slightly overestimates the indices instead of underestimating them. However, PRECIS simulating indices are all closer to the indices derived from APHRODITE. Therefore, PRECIS makes a remarkable improvement in reproducing the historical precipitation compared with its driving GCM. It is further proved that high-resolution simulation is essential to obtain the plausible distribution of precipitation over China. A faithful reproduction of historical climate is the premise for projecting a plausible range of future climate.

Increasing observational and climate modelling studies have investigated the relationship between atmospheric temperature and rainfall intensity as a basis for projecting changes in daily rainfall extremes, arguing that the intensity should increase following either the Clausius–Clapeyron (CC) relation or Super CC relation over certain ranges of temperature and availability in moisture. As shown in Fig. 8, both models reproduce the CC scaling of daily precipitation extremes under 14 °C and the supper CC rate of extremes above 15 °C up to 22 °C reasonably well for the 90th, 99th and 99.9th percentiles. There are subtle differences between the two models for temperature above 22 °C. HadGEM2-ES appears to retain the super CC scaling, whereas the PRECIS model simulates a strong reduction in precipitation intensity. The strong reduction in modeled precipitation intensity

Fig. 8 Dependencies of different extreme percentiles (90th–99.9th) of the distribution of daily precipitation on temperature in three dataset (HadGEM2-ES, PRECIS, and APHRODITE)

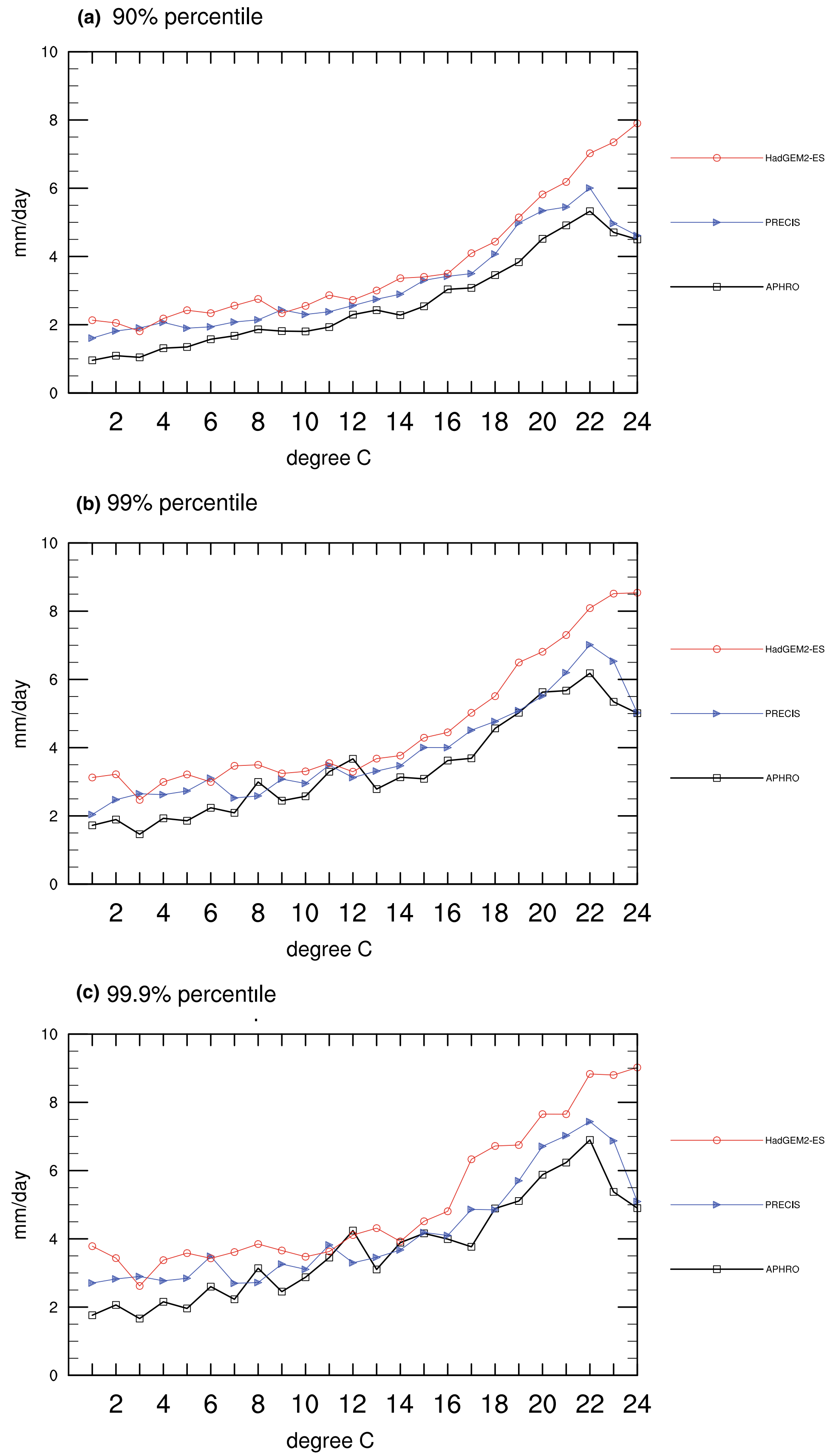

for temperatures above 22 °C is associated with a deficit in atmospheric moisture content, but this relationship is yet to be understood. Relations between temperature and precipitation are difficult to asses because of an ambiguity of causes and effects, in particular over moisture-limited regions and the summer season (Trenberth and Shea 2005). Most important is the dependency of both temperature and precipitation on the atmospheric circulation conditions (Lenderink and Meijgaard 2009). For temperatures above 22 °C, anomalous atmospheric conditions (e.g. with severe soil drying and/or strong high pressure systems) is likely to suppress the occurrence and intensity of precipitation extremes. High pressure systems could cause warm weather with at the same time low relative humidity and low precipitation amounts. A prolonged period with dry weather could result in soil moisture depletion, with further reduced surface evaporation and temperature increases (Vautard et al. 2007). This again implies a negative correlation between temperature and precipitation, which could also be further enhanced by feedbacks from clouds. Moreover, in the observations there are is a fall off in precipitation intensity with increase in the highest temperature range. It is interesting that the PRECIS model discussed here employs a closure of the convection scheme based on moisture convergence (Wilson et al. 2015). Results show that this closure led to a strong positive feedback with soil drying leading to a reduction in precipitation, opposing the results of HadGEM2-ES that gave rise to a negative soil moisture feedback. Therefore, the results exhibit a reference for adding values to its driving GCM by catching fine-scale physical process.

4 Projections of future precipitation

In Fig. 9, it shows the projected precipitation changes relative to the baseline period for HadGEM2-ES and PRECIS under RCP4.5 and RCP8.5 scenarios for the period 2036–2065 (2050s) and the period 2070–2099 (2080s). For the 2050s, both models project a general increase in the annual precipitation over most parts of China under both scenarios. HadGEM2-ES simulates less precipitation in northern sub-regions (northwest China, northcentral China and northeast China) than southern sub-regions (Tibet and south China). However, PRECIS gives an opposite spatial pattern where northern sub-regions have larger increment than southern sub-regions. For northern sub-regions, their relatively high latitudes make them receive more positive albedo-temperature feedback. Therefore, the northern sub-regions have higher temperature increase than the southern sub-regions (Li et al. 2011a, b). Due to a rise in air temperature, water vapor in the atmosphere increases nonlinearly with temperature. This increase in precipitable water is, to first order, responsible for the increase in precipitation, particularly in middle to high latitudes. As for Tibet, melting of the ice and snow cover in the high-elevation areas under warming climate increases water vapor which traps more heat in the surface, and makes the surface less reflective and adds to the warming effect (Hewitson et al. 2014). Hence, it is associated with an establishment of a large-scale thermal contrast between the Asian land mass and neighboring oceans (Li et al. 2008; Li and Yanai 1996; Wu et al. 2012). However, in the air above, models consistently project enhanced upper-tropospheric warming in the tropics (Meehl et al. 2007). This is related to increasing condensational heating in the future climate. The upper-troposphere over the Indian Ocean warms more than over the Tibetan plateau, reducing the meridional thermal gradient between the Asian continent and adjacent oceans, thus leading to a weakening of the Asian monsoon circulation (Ueda et al. 2006). Therefore, less precipitation should be projected in the southern sub-regions than in the northern sub-regions. The results provide a useful reference for identifying the added value of high-resolution model over its low-resolution counterpart in terms of precipitation projection.

Under RCP4.5, PRECIS projects the maximum positive changes taking place in northwest China. These results derived from PRECIS are in consistence with the results of Bao's research on WRF driven by GFDL-ESM2G and Gao's research on RegCM driven by FvGCM over China (Gao et al. 2008; Bao et al. 2015). For the 2080s, the area with maximum annual precipitation change remains the same location for two models but becomes larger than it in the 2050s. Under each representative concertation pathway scenario, it also has been found that the positive precipitation changes are increasing from the 2050s to the 2080s. Figure 10 demonstrates the area-averages of precipitation changes and their differences between RCP4.5 and RCP8.5 for five sub-regions. Through the comparison between the results under two RCPs, the changes in Northwest and Northcentral China are more sensitive to the increase in the radiative forcing for both models, especially in winter. It is possible that the enhanced warming under RCP8.5 reduces the thermal contrast between the Asian land mass and neighboring oceans in wintertime. Therefore, northern sub-regions will experience a weak winter monsoon, which prevents cold-dry air from high latitudes. For South China, HadGEM2-ES models the precipitation with a low sensitivity to the high radiative forcing scenario, whereas PRECIS simulates the precipitation a relatively strong response to the radiative forcing increase and has all negative changes for both season in the 2080s. As for precipitation changes in winter and summer, it is evident that precipitation increases in winter are greater than increases in summer, especially for HadGEM2-ES. Also, a downward trend from north to south over the landmass of China is detected in the output of PRECIS for both seasons, and an opposite trend from

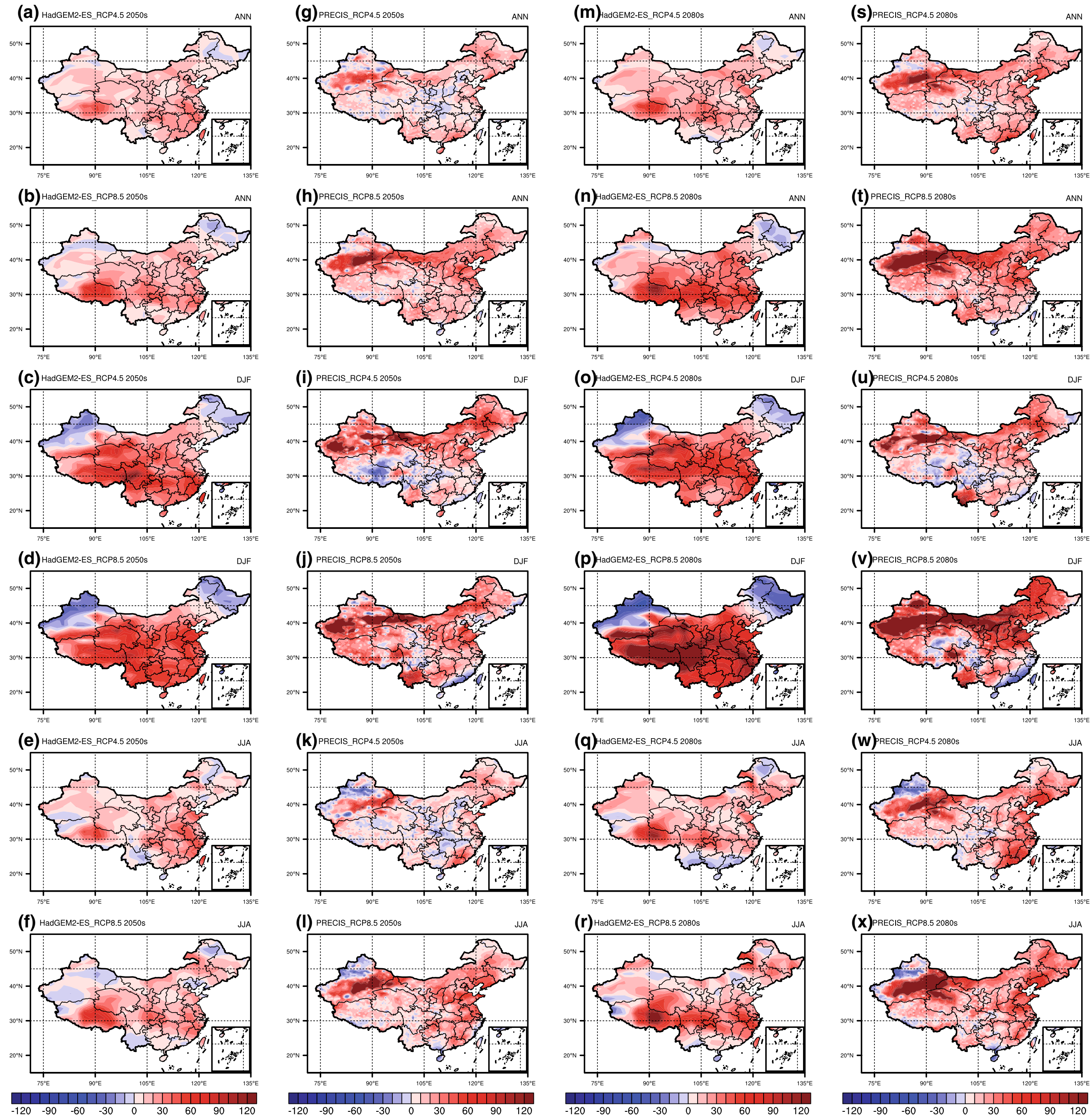

Fig. 9 Spatial distributions of percentage changes for two future periods (2036–2065 relative to 1976–2005 and 2070–2099 relative to 1976–2005) of annual, winter, and summer mean precipitation (unit: %) as projected by HadGEM2-ES and PRECIS

south to north is found in the output of HadGEM2-ES in winter. This result is consistent with the studies on the precipitation associated with climate warming in China (Piao et al. 2010; Liu et al. 2013; Sun and Ao 2013; Zhou et al. 2014). They found that the coupling relationship of winter precipitation and climate warming over China can be physically explained via the East Asian winter monsoon (EAWM) variability. Previous studies have shown that the EAWM experienced an abrupt decadal change around the mid-1980s (Wang and He 2012), after which it became weaker, the weakening of the EAWM during the past several decades could be related to climate warming, because simulations of coupled climate models show that the EASM will decrease under the warming background (Hori and Ueda 2006). The weakened EAWM further weakens the control of its related cold-dry air over East Asia, favouring the northward flow

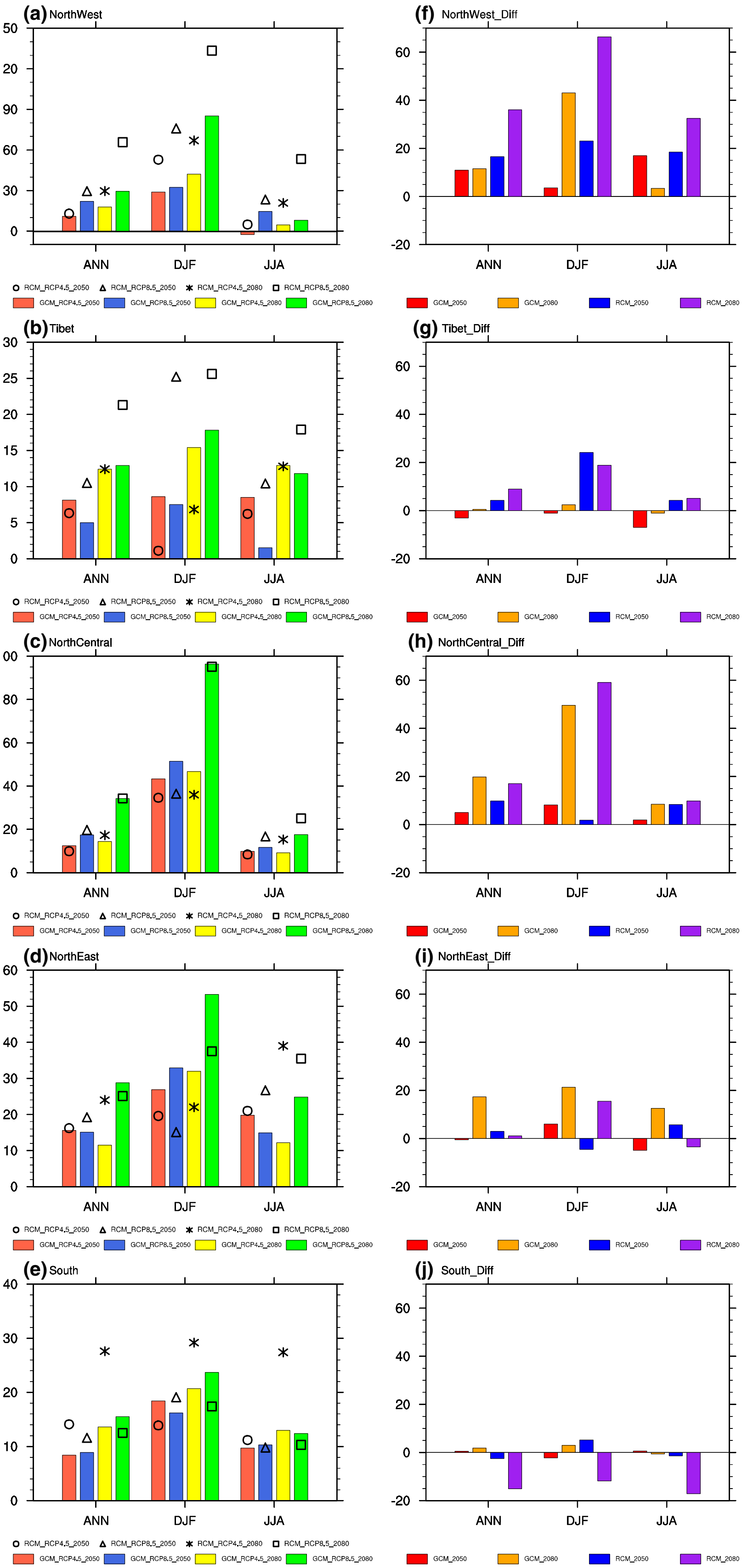

Fig. 10 Future percentage changes (2036–2065 relative to 1976–2005 and 2070–2099 relative to 1976–2005) of annual, winter, and summer mean precipitation (unit: %) for HadGEM2-ES and PRECIS over the five sub-regions under RCP4.5 and RCP8.5

of warm-moist air from low latitudes and the ocean. Consequently, in a weaker EAWM year, there is more winter precipitation over China (Zhou 2011). These results are consistent with the distribution of winter precipitation and extreme precipitation associated with climate warming in China. The quantitative analysis shows that both winter and summer precipitation and extreme precipitation are increasing, however, the rate of increase in summer is less than that in winter. These results indicate that the response of precipitation and extreme precipitation is stronger in winter, the season with greater warming, which further suggests that investigating the seasonal impact of warming offers more comprehensive data.

Temporal changes in the frequencies of precipitation intensities under RCP4.5 and RCP 8.5 between future periods and the reference period are shown in Fig. 11. For all five sub-regions, both PRECIS and HadGEM2-ES have negative changes in the frequencies of precipitation intensities below 5 mm/day and positive changes in the frequencies of precipitation intensities above 15 mm/day under no matter which radiative concentration pathway scenario for both periods. The above results suggest a shift of the precipitation distribution from light to intense precipitation together across the whole of China. Studies indicate that this is primarily due to the contribution of radiative forcing increased by Green House Gas (GHG). GHG-induced warming increases the water holding capacity of the atmosphere and thus increases atmospheric precipitable water. As the atmosphere becomes more stable with more moisture, the frequency of precipitating events decreases, but the precipitation intensity can be stronger once an event occurs because more moisture is available in a warmer atmosphere. Furthermore, the observed changes are qualitatively consistent with model projected changes under increasing radiative forcing (Sun et al. 2007; Chou and Lan 2012; Ma et al. 2015), although we should note that the observed changes of precipitation in China are significantly affected by internal climate variability (Dong et al. 2014). Zhou et al. distinguished that the changes in precipitation characteristics more due to external radiative forcing than internal climate variability (Zhou et al. 2013). Overall, most results of PRECIS are consistent with its driving GCM for temporal changes over five sub-regions. However, there are some inconsistencies between two models for the frequencies of precipitation intensities from 5 to 30 mm/day over the southern sub-regions. PRECIS projects positive changes in the frequencies of precipitation intensities between 5 and 30 mm/day, while HadGEM2-ES projects negative changes among that range over Tibet and south China. PRECIS simulates a more violent alteration in the temporal changes in the frequencies of precipitation intensities than HadGEM2-ES does. From the 2050s to the 2080s, different trends are detected in the temporal changes derived from PRECIS and HadGEM2-ES for five sub-regions.

Figure 12 shows the projected changes relative to the reference period in the indices of precipitation extremes over China under RCP4.5 and RCP8.5 for two future periods. Regional statistics for projected changes relative to the baseline period in indices of precipitation extremes and comparison between results under RCP4.5 and under RCP8.5 for two future periods are displayed in Fig. 13. As shown in Figures, most markers are above 0 for R95p, R99p and SDII which means both models simulate an increase in three indices over China under both scenarios for two periods. A widespread increase of R95p was also projected over China by using RegCM4 to downscale BCC-CSM1.1. under the RCPs scenario (Ji and Kang 2015). Results from R99p have the similar spatial distribution with R95p, but the magnitude of maximum change is up to 10%. The projected SDII change pattern is very similar to the result derived by using RegCM3 to downscale the CCSR/NIES/FRCGC/MORPC3.2_hires under A1B (Xu et al. 2013). With increase in the radiative forcing, both models simulate positive changes of R95p, R99p and SDII in most sub-regions, except negative changes simulated by PRECIS in south China and northeast China in 2080s. As for WDF and CWD, both models tend to have markers below 0 for northeast China and south China. Therefore, the extreme precipitation amounts in northeast China and south China are projected to increase while the frequencies of their extreme precipitation are decreasing for both models. It suggests that the future daily extreme precipitation intensities are likely to become large in northeast China and south China. Researchers also found that the frequency of precipitating events decreases (CWD decreases), but the precipitation intensity can be stronger once an event occurs because more moisture is available in a warmer atmosphere (Kitoh and Hirokazu 2016; Zou et al. 2016). In WDF, changes are increased by the increment in radiative forcing for the northern sub-regions and decreased for the southern sub-regions for PRECIS. As for HadGEM2-ES, only changes over Tibet, northeast China and south China in the 2050s are decreased by the radiative forcing increasing. Under both RCPs, HadGEM2-ES projects an increase in CWD over Tibet and northwest China for both periods. Compare to the results under RCP4.5, HadGEM2-ES tends to simulate CWD with lower values under RCP8.5. PRECIS, however, simulates negative changes in CWD over most parts of China, particularly in the three northern sub-regions. The CWD modeled by PRECIS is relatively less sensitive to the increase in the radiative forcing compared with its driving GCM.

5 Conclusions

In this study, the high-resolution model PRECIS driven by HadGEM2-ES was used to downscale the historical and two

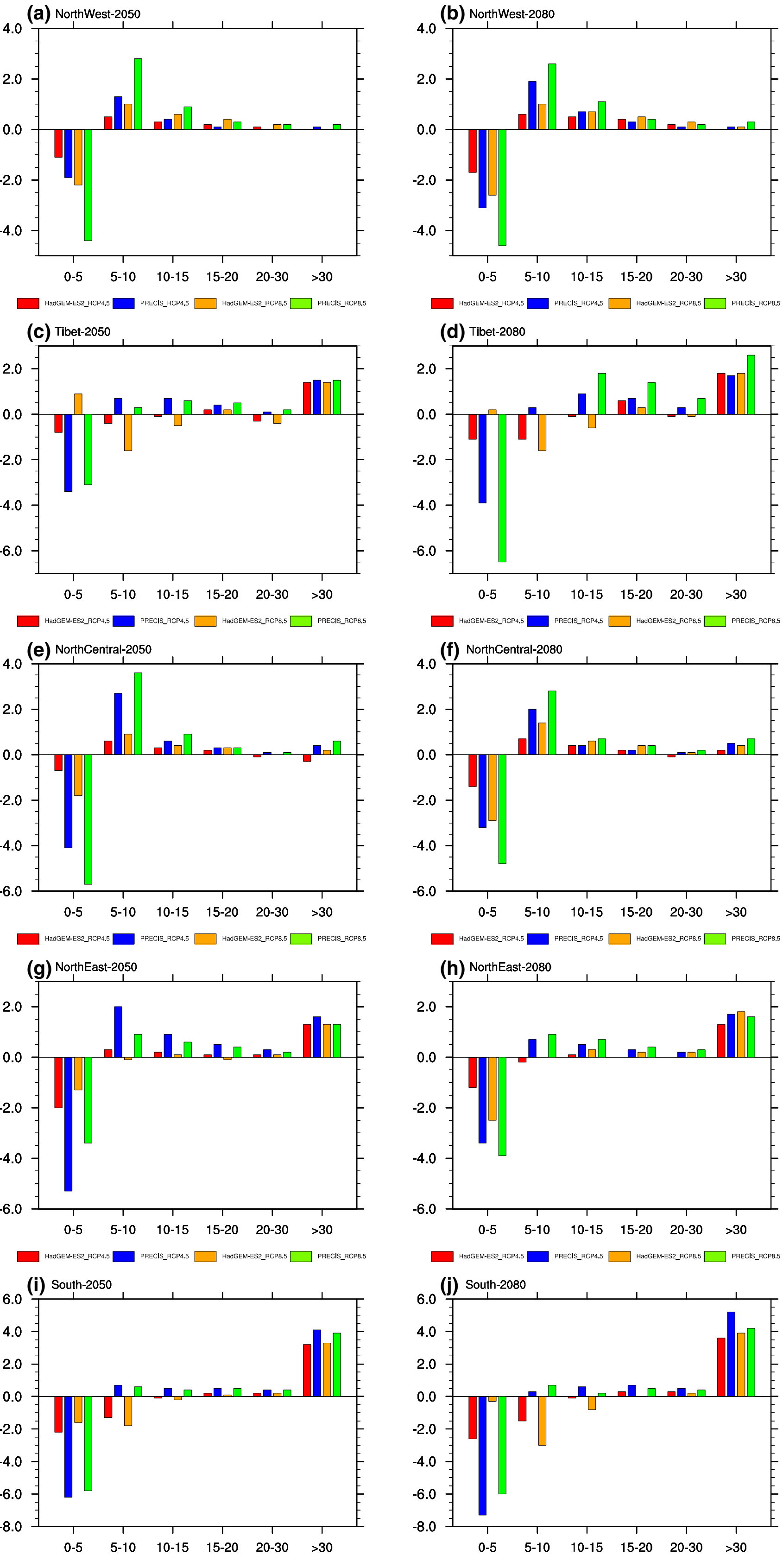

Fig. 11 Temporal changes in the frequencies of precipitation intensities (unit: %) between two future periods (2036–2065 and 2070–2099) and the reference period (1976–2005) as projected by HadGEM2-ES and PRECIS

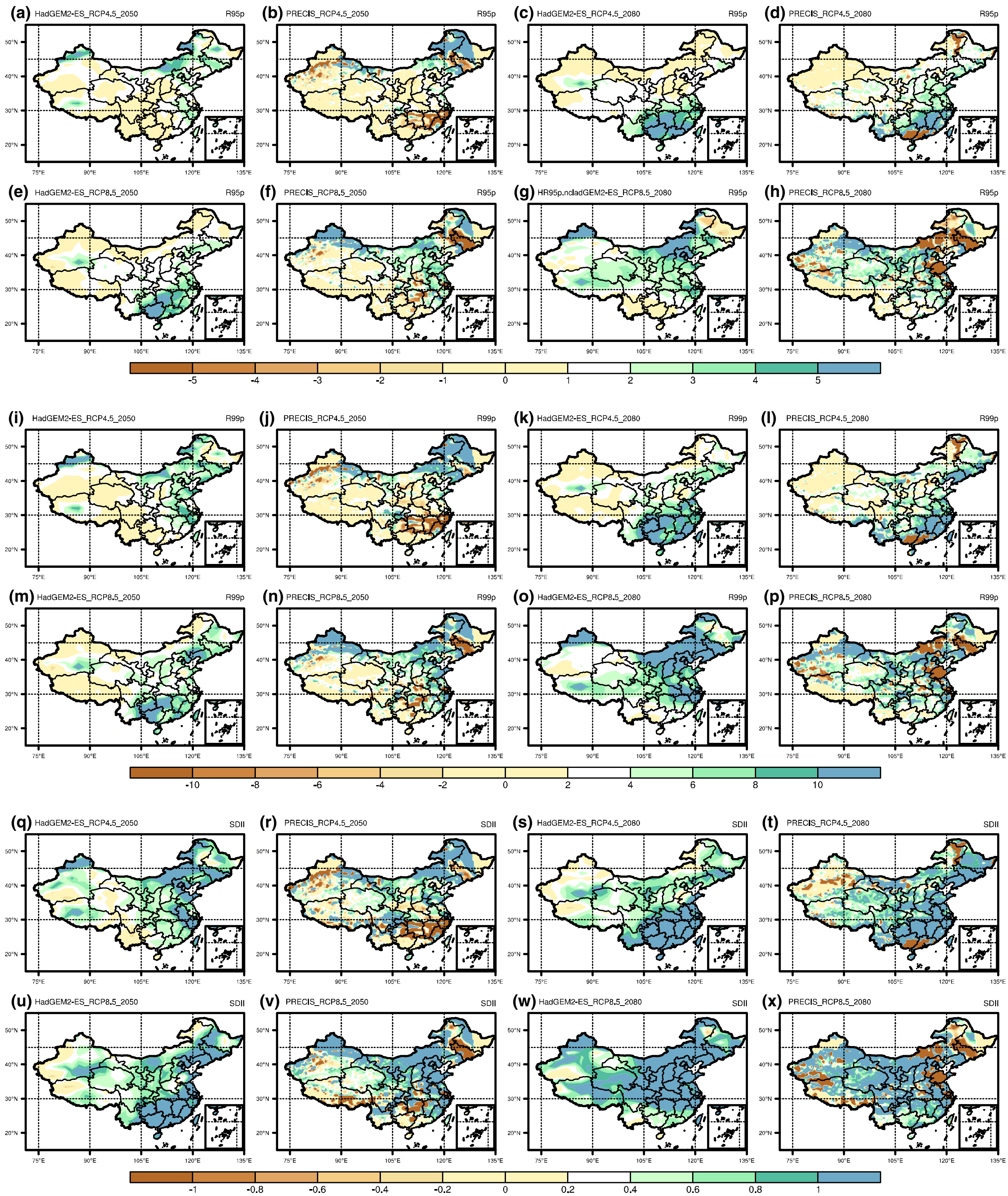

Fig. 12 Spatial distributions of projected changes in the indices of precipitation extremes (R95p, unit: %; R99p, unit: %; SDII, unit: mm/day; WDF, unit: %; and CWD, unit: days) between two future periods (2036–2065 and 2070–2099) and the baseline period over China under RCP4.5 and RCP8.5 as projected by HadGEM2-ES and PRECIS

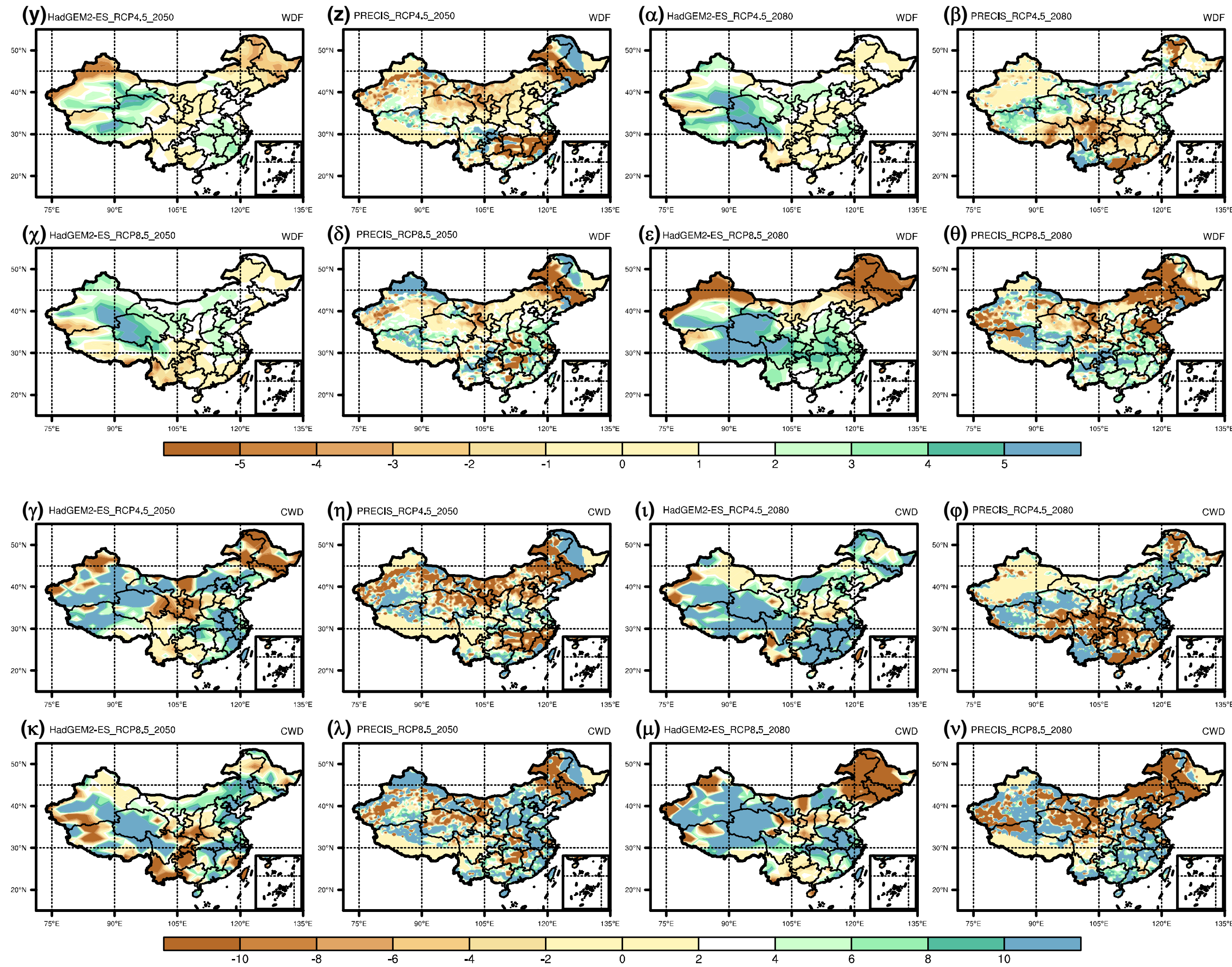

Fig. 12 (continued)

future periods' precipitation and extremes under RCP4.5 and RCP8.5 over China. First, this study examines the performances of both models on simulating the historical climate for the baseline period from 1976 to 2005. The PRECIS model is capable of simulating precipitation and the related extremes, and reproducing their spatial distributions over China. The PRECIS model also captures the regional features in observations and exhibits more reasonable regional averages of indices of precipitation extremes. With improved resolution, the PRECIS model is capable of better representing the fine-scale physical process than HadGEM2-ES. It can provide reliable spatial patterns of precipitation and extremes with high spatial correlations to observations. In terms of temporal distribution, both the annual cycle and the frequency of daily precipitation intensity simulated by PRECIS agree well with the observation. Through the discussion and analysis, it further proves that dynamical downscaling adds values to regional simulation in the mean precipitation and extreme precipitation with physical explanations. All of the above points to the importance of using a high-resolution regional climate model to represent the historical precipitation better and provide reliable projections for the future precipitation and extremes over China.

Under RCP4.5 and RCP8.5, both models project the precipitation increased over most parts of China for two future periods. The projected maximum change in the annual mean precipitation is about 1.5 times of that for the baseline period. Precipitation changes in winter are greater than changes in summer for both models. The PRECIS model simulates a more violent alteration in the temporal changes in the frequencies of precipitation intensities than HadGEM2-ES does. The radiative forcing increasing from RCP4.5 to RCP8.5 intensifies the precipitation changes for two models in the 2050s and the 2080s. Under each representative concertation pathway scenario, it also has been found that the positive precipitation changes are increased from the 2050s

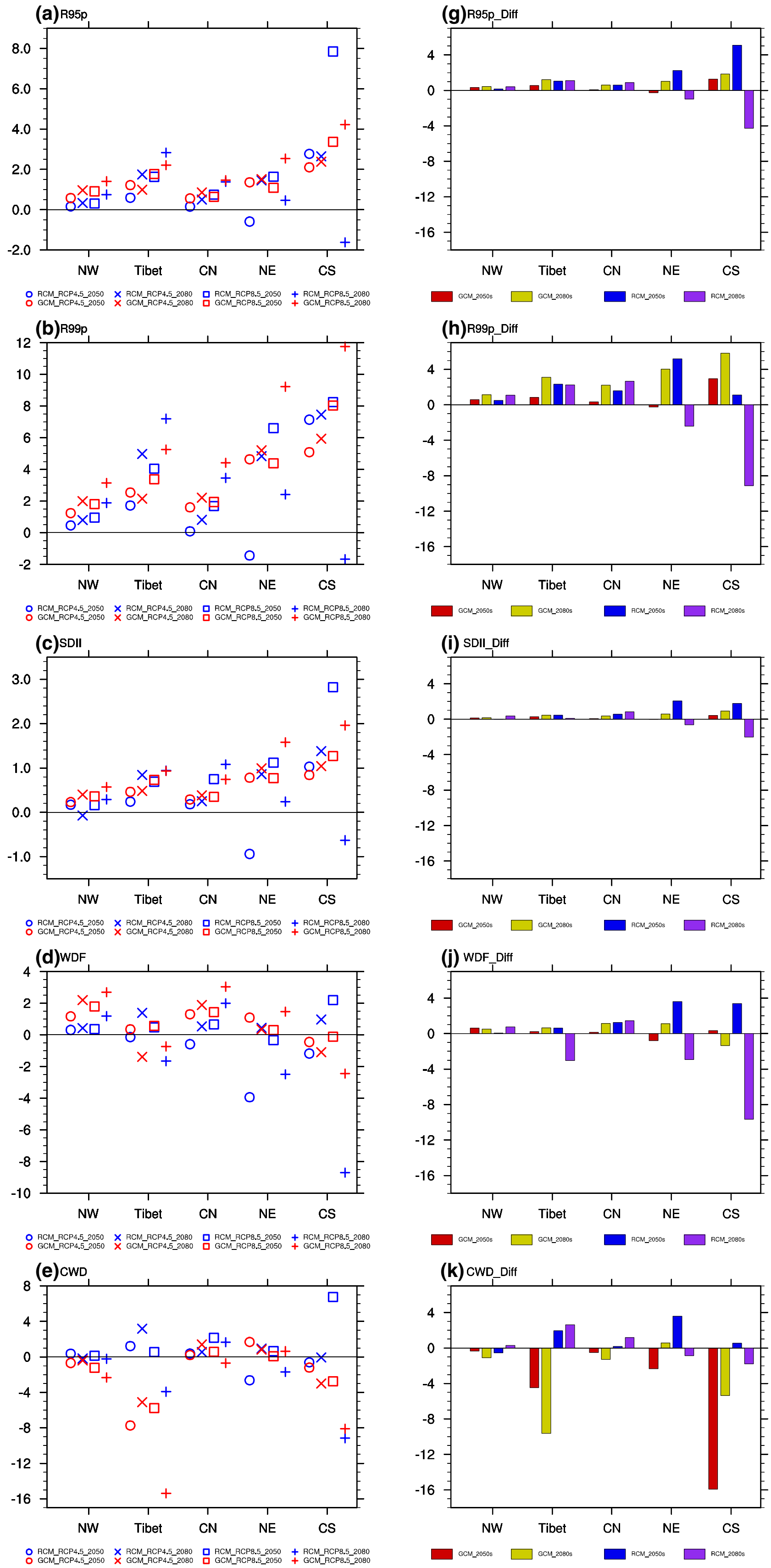

Fig. 13 Projected changes in indices of precipitation extremes (R95p, unit: %; R99p, unit: %; SDII, unit: mm/day; WDF, unit: %; and CWD, unit: days) between two future periods (2036–2065 and 2070–2099) and the baseline period over China under RCP4.5 and RCP8.5 as projected by HadGEM2-ES and PRECIS

to the 2080s. Both models have the geographical differences in projected precipitation changes as is evident that three northern sub-regions have larger magnitudes of precipitation changes than the two southern sub-regions. For all five sub-regions, both PRECIS and HadGEM2-ES project negative changes in the frequencies of precipitation intensities below 5 mm/day and positive changes in the frequencies of precipitation intensities above 15 mm/day under both RCPs for the two future periods. Especially, frequencies of precipitation intensities above 30 mm/day are found with a high rise over northeast China, Tibet, and south China.

Analysis of changes in the indices of precipitation extremes relative to the baseline period indicates that both models simulate an increase in R95p, R99p, and SDII over China under both scenarios for two periods. Both models tend to have negative changes in WDF and CWD over northeast China and south China. The increased extreme precipitation amounts accompanied with decreased frequencies of their extreme precipitation suggests that the future daily extreme precipitation intensities are likely to become large in northeast China and south China for both models. For five sub-regions, their changes have a growing trend in R95p, R99p and SDII, and an opposite trend in CWD from the 2050s to the 2080s. As radiative forcing increasing from RCP4.5 to RCP8.5, HadGEM2-ES intensifies the changes in R95p, R99p and SDII for all sub-regions; intensifies the changes in WDF over the northern sub-regions and diminishes the changes over the southern sub-regions; diminishes the changes in CWD as a whole for the five regions.

References

Bao J, Feng J, Wang Y (2015) Dynamical downscaling simulation and future projection of precipitation over China. J Geophys Res Atmos 120:8227–8243. doi:10.1002/2015JD023275

Bucchignani E, Montesarchio M, Cattaneo L, Manzi MP, Mercogliano P (2014), Regional climate modeling over China with COSMO-CLM: performance assessment and climate projections. J Geophys Res Atmos 119:12151–12170. doi:10.1002/2014JD022219

Chen L, Frauenfeld OW (2014) A comprehensive evaluation of precipitation simulations over China based on CMIP5 multimodel ensemble projections. J Geophys Res Atmos 119:5767–5786. doi:10.1002/2013JD021190

Chen H, Sun J (2009) How the "best" models project the future precipitation change in China. Adv Atmos Sci 26(4):773–782. doi:10.1007/s00376-009-8211-7

Chou C, Lan C (2012) Changes in the annual range of precipitation under global warming. J Clim 25:222–235. doi:10.1175/JCLI-D-11-00097.1

Christensen JH et al (2007) Regional climate projections, in climate change 2007: the physical science basis. In: Solomon S et al (eds) Contribution of working group i to the fourth assessment report of the intergovernmental panel on climate change. Cambridge University Press, Cambridge, pp 847–940

Colette A, Vautard R, Vrac M (2012) Regional climate downscaling with prior statistical correction of the global climate forcing. Geophys Res Lett 39:L13707. doi:10.1029/2012GL052258

Collins WJ, Bellouin N, Doutriaux-Boucher M, Gedney N, Hinton T, Jones CD, Liddicoat S, Martin G, O'Connor F, Rae J, Senior C, Totterdell I, Woodward S, Reichler T, Kim J (2008), Evaluation of the HadGEM2 model. Met Office Hadley Centre Technical Note no. HCTN 74, available from Met Office, FitzRoy Road, Exeter EX1 3 PB. http://www.metoffice.gov.uk/publications/HCTN/index.html. Accessed 24 Oct 2016

Dong L, Zhou T, Chen X (2014) Changes of Pacific decadal variability in the twentieth century driven by internal variability, greenhouse gases, and aerosols. Geophys Res Lett 41:8570–8577. doi:10.1002/2014GL062269

Dunne JP et al (2012) GFDL's ESM2 global coupled climate–carbon Earth system models. Part I: Physical formulation and baseline simulation characteristics. J Clim 25:6646–6665. doi:10.1175/JCLI-D-11-00560.1

Ehret U, Zehe E, Wulfmeyer V, Warrach-Sagi K, Liebert J (2012) HESS Opinions "Should we apply bias correction to global and regional climate model data? Hydrol Earth Syst Sci 16:3391–3404. doi:10.5194/hess-16-3391-2012

Feng L, Zhou T, Wu B, Li T, Luo J (2011) Projection of future precipitation changes over China with a high-resolution global atmospheric model. Adv Atmos Sci 28(2):464–476. doi:10.1007/s00376-010-0016-1

Feng J, Wang Y, Ma Z, Liu Y (2012) Simulating the regional impacts of urbanization and anthropogenic heat release on climate across China. J Clim 25(20):7187–7203. doi:10.1175/JCLI-D-11-00333.1

Flato G et al (2013) Evaluation of climate models. In: Stocker TF et al (eds) Climate change 2013: the physical science basis. contribution of working group I to the fifth assessment report of the intergovernmental panel on climate change. Cambridge University Press, Cambridge, pp 741–866

Frich P, Alexander LV, Della-Marta P, Gleason B, Haylock M, Klein Tank AMG, Peterson T (2002) Observed coherent changes in climatic extremes during the second half of the twentieth Century. Clim Res 19:193–212

Gao X, Zhao Z, Ding Y, Huang R, Giorgi F (2001) Climate change due to greenhouse effects in China as simulated by a regional climate model. Adv Atmos Sci 18:1224–1230. doi:10.1007/s00376-001-0036-y

Gao X, Shi Y, Song R, Giorgi F, Wang Y, Zhang D (2008) Reduction of future monsoon precipitation over China: comparison between a high-resolution RCM simulation and the driving GCM. Meteorol Atmos Phys 100:73–86. doi:10.1007/s00703-008-0296-5

Gao X, Shi Y, Giorgi F (2011) A high resolution simulation of climate change over China. Sci China Earth Sci 54(3):462–472. doi:10.1007/s11430-010-4035-7

Gao X, Shi Y, Zhang D, Wu J, Giorgi F, Ji Z, Wang Y (2012) Uncertainties in monsoon precipitation projections over China: results from two high-resolution RCM simulations. Clim Res 52:213–226. doi:10.3354/cr01084

Gao X-J, Wang M-L, Giorgi F (2013) Climate change over China in the 21st century as simulated by BCC_CSM1.1-RegCM4.0. Atmos Ocean Sci Lett 6(5):381–386. doi: 10.3878/j.issn.1674-2834.13.0029

Giorgi F (2006) Regional climate modeling: status and perspectives. J Phys IV 139:101–118. doi:10.1051/jp4:2006139008

Giorgi F, Mearns LO (1991) Approaches to the simulation of regional climate change: A review. Rev Geophys 29:191–216. doi:10.1029/90RG02636

Giorgi F, Jones J, Asrar GR (2009) Addressing climate information needs at the regional level: the CORDEX framework. WMO Bull 58(3):175–183

Gong H, Wang L, Chen W, Wu R, Wei K, Cui X (2014) The climatology and interannual variability of the East Asian winter monsoon in CMIP5 models. J Clim 27(4):1659–1678. doi:10.1175/JCLI-D-13-00039.1

Guo J, Huang G, Wang X, Li Y, Lin Q (2017) Investigating future precipitation changes over China through a high-resolution regional climate model ensemble. Earth's Future 5:285–303. doi:10.1002/2016EF000433

Hartmann DL et al (2013) Observations: atmosphere and surface, in climate change 2013: the physical science basis. In: Stocker TF et al (eds) Contribution of working group i to the fifth assessment report of the intergovernmental panel on climate change. Cambridge Univ. Press, Cambridge, pp 159–254

Held IM, Soden BJ (2006) Robust responses of the hydrological cycle to global warming. J Clim 19:5686–5699. doi:10.1175/JCLI3990.1

Hewitson B, Janetos AC, Carter TR, Giorgi F, Jones RG, Kwon W-T, Mearns LO, Schipper ELF, van Aalst M (2014), Regional context, in climate change 2014: impacts, adaptation, and vulnerability. Part B: regional aspects. Contribution of working group II to the fifth assessment report of the intergovernmental panel on climate change, In: Barros VR et al (eds) Climate change 2014: impacts, adaptation, and vulnerability. Cambridge University Press, Cambridge, pp 1133–1197

Hirakuchi H, Giorgi F (1995), Multi-year present day and 2x CO_2 simulations of monsoon-dominated climate over eastern Asia and Japan with a regional climate model nested in a general circulation model. J Geophys Res. 100:21105–21,125. doi:10.1029/95JD01885

Hori ME, Ueda H (2006) Impact of global warming on the East Asian winter monsoon as revealed by nine coupled atmosphere–ocean GCMs. Geophys Res Lett 33:L03713. doi:10.1029/2005GL024961

Huang DQ, Zhu J, Zhang YC, Huang AN (2013) Uncertainties on the simulated summer precipitation over eastern China from the CMIP5 models. J Geophys Res Atmos 118:9035–9047. doi:10.1002/jgrd.50695

Ji Z, Kang S (2015) Evaluation of extreme climate events using a regional climate model for China. Int J Climatol 35:888–902. doi:10.1002/joc.4024

Jiang L, Yan Y, Hararuk O, Mikle N, Xia J, Shi Z, Tjiputra J, Wu T, Luo Y (2015) Scale-dependent performance of CMIP5 earth system models in simulating terrestrial vegetation carbon. J Clim 28:5217–5232. doi: 10.1175/JCLI-D-14-00270.1

Jones RG, Noguer M, Hassell DC, Hudson D, Wilson SS, Jenkins GJ, Mitchell JFB (2004) Generating high resolution climate change scenarios using PRECIS. Met Office Hadley Centre, Exeter (40 pp, April 2004)

Karl TR, Knight RW, Plummer N (1995) Trends in high-frequency climate variability in the twentieth century. Nature 377:217–220. doi:10.1038/377217a0

Kitoh A, Hirokazu E (2016), Changes in precipitation extremes projected by a 20-km mesh global atmospheric model. Weather Clim Extremes. doi:10.1016/.j.wace.2015.09.001

Kitoh A, Endo H, Krishna Kumar K, Cavalcanti IFA, Goswami P, Zhou T (2013) Monsoons in a changing world: a regional perspective in a global context. J Geophys Res Atmos 118:3053–3065. doi:10.1002/jgrd.50258

Lee JW, Hong SY, Chang EC, Suh MS, Kang HS (2014) Assessment of future climate change over East Asia due to the RCP scenarios downscaled by GRIMs-RMP. Clim Dyn 42(3–4):733–747. doi:10.1007/s00382-013-1841-6

Lenderink G, Meijgaard E (2009) Reply to: unexpected rise in extreme precipitation caused by a shift in rain type? Nat Geosci 2:373. doi:10.1038/ngeo524

Li C, Yanai M (1996) The onset and interannual variability of the Asian summer monsoon in relation to land-sea thermal contrast. J Clim 9:358–375. doi:10.1175/1520-0442(1996)009<0358:TOAIVO>2.0.CO;2

Li S, Lu J, Huang G, Hu K (2008) Tropical Indian Ocean basin warming and East Asian summer monsoon: a multiple AGCM study. J Clim 21:6080–6088. doi: 10.1175/2008JCLI2433.1

Li H, Feng L, Zhou T (2011a) Multi-model projection of July–August climate extreme changes over China under CO_2 doubling. Part I: Precipitation. Adv Atmos Sci 28(2):433–447. doi:10.1007/s00376-010-0013-4

Li HM, Feng L, Zhou TJ (2011b) Multi-model projection of July–August climate extreme changes over China under CO_2 doubling. Part II: Temperature. Adv Atmos Sci 28(2):448–463. doi:10.1007/s00376-010-0052-x

Li Z, Lau WK-M, Ramanathan V, Wu G, Ding Y, Manoj MG, Liu J, Qian Y, Li J, Zhou T, Fan J, Rosenfeld D, Ming Y, Wang Y, Huang J, Wang B, Xu X, Lee S-S, Cribb M, Zhang F, Yang X, Zhao C, Takemura T, Wang K, Xia X, Yin Y, Zhang H, Guo J, Zhai PM, Sugimoto N, Babu SS, Brasseur GP (2017) Aerosol and monsoon climate interactions over Asia. Rev Geophys 54:866–929. doi:10.1002/2015RG00050

Liang XZ, Kunkel KE, Meehl GA, Jones RG, Wang JX (2008) Regional climate models downscaling analysis of general circulation models present climate biases propagation into future change projections. Geophys Res Lett 35:L08709. doi:10.1029/2007GL032849

Liu S, Gao W, Liang XZ (2013) A regional climate model downscaling projection of China future climate change. Clim Dyn 41(7–8):1871–1884. doi:10.1007/s00382-012-1632-5

Luo L, Tang W, Lin Z et al (2013) Evaluation of summer temperature and precipitation predictions from NCEP CFSv2 retrospective forecast over China. Clim Dyn 41:2213–2230. doi:10.1007/s00382-013-1927-1

Ma S, Zhou T, Dai A, Han Z (2015) Observed changes in the distributions of daily precipitation frequency and amount over China from 1960 to 2013. J Clim 28:6960–6978. doi: 10.1175/JCLI-D-15-0011.1

Ma S, Zhou T, Stone DA, Polson D, Dai A, Stott PA, von Storch H, Qian Y, Burke C, Wu P, Zou L, Ciavarella A (2017) Detectable anthropogenic shift toward heavy precipitation over Eastern China. J Clim 30:1381–1396. doi: 10.1175/JCLI-D-16-0311.1

MACA (2017) MACA Downscaling of CMIP5 GCMs, multivariate adaptive constructed analogs (MACA) datasets. http://maca.northwestknowledge.net/GCMs.php. Accessed 14 May 2017

Martin GM, Bellouin N, Collins WJ et al (2011) The HadGEM2 family of met office unified model climate configurations. Geosci Model Dev 4(3):723–757. doi:10.5194/gmd-4-723-2011

Meehl GA et al (2007) Global climate projections. in climate change 2007: the physical science basis. In: Solomon S et al (eds) Contribution of working group I to the fourth assessment report of the intergovernmental panel on climate change. Cambridge University Press, Cambridge, pp 747–845

Moss RH et al (2010) The next generation of scenarios for climate change research and assessment. Nature 463(7282):747–756. doi:10.1038/nature08823

Mulcahy JP, Walters DN, Bellouin N, Milton SF (2014) Impacts of increasing the aerosol complexity in the met office global numerical weather prediction model. Atmos Chem Phys 14:4749–4778. doi:10.5194/acp-14-4749-2014

Piao S, Ciais P, Huang Y et al (2010) The impacts of climate change on water resources and agriculture in China. Nature 467:43–51. doi:10.1038/nature09364

Racherla PN, Shindell DT, Faluvegi GS (2012) The added value to global model projections of climate change by dynamical downscaling: a case study over the continental US using the GISS-ModelE2 and WRF models. J Geophys Res 117:D20118. doi:10.1029/2012JD018091

Rupp DE, Abatzoglou JT, Hegewisch KC, Mote PW (2013), Evaluation of CMIP5 20th century climate simulations for the Pacific Northwest USA., J Geophys Res Atmos 118:10884–10906. doi:10.1002/jgrd.50843

Sato T, Xue Y (2013) Validating a regional climate model's downscaling ability for East Asian summer monsoonal interannual variability. Clim Dyn 41:2411–2426. doi:10.1007/s00382-012-1616-5

Seager R et al (2007) Model projections of an imminent transition to a more arid climate in southwestern North America. Science 316(5828):1181–1184. doi:10.1126/science.1139601

Sperber KR, Annamalai H, Kang IS, Kitoh A, Moise A, Turner A, Wang B, Zhou T (2013) The Asian summer monsoon: an intercomparison of CMIP5 vs. CMIP3 simulations of the late 20th century. Clim Dyn 41(9–10):2711–2744. doi:10.1007/s00382-012-1607-6

Sun J, Ao J (2013) Changes in precipitation and extreme precipitation in a warming environment in China. J China Sci Bull 58:1395. doi:10.1007/s11434-012-5542-z

Sun Y, Solomon S, Dai A, Portmann RW (2007) How often will it rain? J Clim 20:4801–4818. doi:10.1175/JCLI4263.1

Sun Q, Miao C, Duan Q (2015) Comparative analysis of CMIP3 and CMIP5 global climate models for simulating the daily mean, maximum, and minimum temperatures and daily precipitation over China. J Geophys Res Atmos 120:4806–4824. doi:10.1002/2014JD022994

Taylor KE (2001) Summarizing multiple aspects of model performance in a single diagram. J Geophys Res 106:7183–7192. doi:10.1029/2000JD900719

Taylor KE, Stouffer RJ, Meehl GA (2012) An overview of CMIP5 and the experiment design. Bull Am Meteorol Soc 93:485–498. doi:10.1175/BAMS-D-11-00094.1

Trenberth KE, Shea DJ (2005) Relationships between precipitation and surface temperature. Geophys Res Lett 32:L14703. doi:10.1029/2005GL022760

Ueda H, Iwai A, Kuwano K, Hori ME (2006) Impact of anthropogenic forcing on the Asian summer monsoon as simulated by eight GCMs. Geophys Res Lett 33:L06703. doi:10.1029/2005GL025336

Van Vuuren DP et al (2011) The representative concentration pathways: An overview. Clim Change 109:5–31. doi:10.1007/s10584-011-0148-z

Vautard R, Yiou P, D'Andrea F, de Noblet N, Viovy N, Cassou C, Polcher J, Ciais P, Kageyama M, Fan Y (2007), Summertime European heat and drought waves induced by wintertime Mediterranean rainfall deficit. Geophys Res Lett 34:L07711. doi:10.1029/2006GL028001

Wang HJ, He SP (2012) Weakening relationship between East Asian winter monsoon and ENSO after mid-1970s. China Sci Bull 57:3535–3540. doi:10.1007/s11434-012-5285-x

Wang XQ, Huang GH, Lin QG, Nie XH, Cheng GH, Fan YR, Li Z, Yao Y, Suo MQ (2013) A stepwise cluster analysis approach for downscaled climate projection—a Canadian case study. Environ Model Softw 49:141–151. doi: 10.1016/j.envsoft.2013.08.006

Wang XQ, Huang GH, Liu JL (2014) Projected increases in near-surface air temperature over Ontario, Canada: a regional climate modeling approach. Clim Dyn. doi: 10.1007/s00382-014-2387-y

Wang XQ, Huang GH, Lin Q, Nie X, Liu JL (2015) High-resolution temperature and precipitation projections over Ontario, Canada: a coupled dynamical-statistical approach. QJR Meteorol Soc 141:1137–1146. doi:10.1002/qj.2421

Wang X, Huang G, Liu J (2016), Twenty-first century probabilistic projections of precipitation over Ontario, Canada through a regional climate model ensemble. Clim Dyn 46:3979. doi:10.1007/s00382-015-2816-6

Wehner MF, Smith RL, Bala G, Duffy P (2010) The effect of horizontal resolution on simulation of very extreme US precipitation events in a global atmosphere model. Clim Dyn 34(2–3):241–247. doi:10.1007/s00382-009-0656-y

White CJ, McInnes KL, Cechet RP, Corney SP, Grose MR, Holz GK, Katzfey JJ, Bindoff NL (2013) On regional dynamical downscaling for the assessment and projection of temperature and precipitation extremes across Tasmania. Aust Clim Dyn 41(11–12):3145–3165. doi:10.1007/s00382-013-1718-8

Wilson W, Hassell D, Hein D, Wang C, Tucker S, Jones R, Taylor R (2015), Technical manual for PRECIS: the met office hadley centre regional climate modelling system version 2.0.0. http://www.metoffice.gov.uk/precis. Accessed 11 Sept 2016

Wood AW, Lettenmaier DP, Palmer RN (1997) Assessing climate change implications for water resources planning. Clim Change 37(1):203–228

Wu G, Liu Y, He B, Bao Q, Duan A, Jin F-F (2012), Thermal controls on the Asian summer monsoon. Sci Rep 2:404. doi:10.1038/srep00404

Xu C-H, Xu Y (2012) The projection of temperature and precipitation over China under RCP scenarios using a CMIP5 multi-model ensemble, Atmos. Ocean Sci Lett 5:527–533

Xu Y, Zhang Y, Lin E, Lin W, Dong W, Jones R, Hassell D, Wilson S (2006) Analyses on the climate change responses over China under SRES B2 scenario using PRECIS. Chin Sci Bull 51:2260–2267. doi:10.1007/s11434-006-2099-8

Xu Y, Gao XJ, Shen Y, Xu CH, Shi Y, Giorgi F (2009) A daily temperature dataset over China and its application in validating a RCM simulation. Adv Atmos Sci 26(4):763–772. doi:10.1007/s00376-009-9029-z

Xu J, Shi Y, Gao X, Giorgi F (2013) Projected changes in climate extremes over China in the 21st century from a high resolution regional climate model (RegCM3). Chin Sci Bull 58:12, 1443–1452. doi:10.1007/s11434-012-5548-6

Xue Y, Janjic Z, Dudhia J, Vasic R, Sales FD (2014), A review on regional dynamical downscaling in inter-seasonal to seasonal simulation/prediction and major factors that affect downscaling ability. Atmos Res 147–148:68–85.doi: 10.1016/j.atmosres.2014.05.001

Yan D, Werners SE, Ludwig F, Huang HQ (2015) Hydrological response to climate change: the pearl river, China under different RCP scenarios. J Hydrol 4(B):228–245. 10.1016/j.ejrh.2015.06.006

Yatagai A, Kamiguchi K, Arakawa O, Hamada A, Yasutomi N, Kitoh A (2012) APHRODITE: constructing a long-term daily gridded precipitation dataset for Asia based on a dense network of rain gauges. Bull Am Meteorol Soc. doi:10.1175/BAMS-D-11-00122.1

Yu E-T, Wang H-J, Sun J-Q (2010) A quick report on a dynamical downscaling simulation over China using the nested model. Atmos Ocean Sci Lett 3:325–329

Yuan X, Liang X-Z, Wood EF (2012) WRF ensemble downscaling seasonal forecasts of China winter precipitation during 1982–2008 Clim Dyn 39(7–8):2041–2058. doi:10.1007/s00382-011-1241-8

Zhang H, Fraedrich K, Blender R, Zhu X (2013) Precipitation extremes in CMIP5 simulations on different time scales. J Hydrometeor 14:923–928. doi: 10.1175/JHM-D-12-0181.1

Zhang X, Liu H, Zhang M (2015) Double ITCZ in coupled ocean–atmosphere models: from CMIP3 to CMIP5. Geophys Res Lett 42:8651–8659. doi:10.1002/2015GL065973

Zheng Z, Gao J, Ma Z, Wang Z, Yang X, Luo X, Jacquet T, Fu G (2016) Urban flooding in China: main causes and policy recommendations. Hydrol Process 30:1149–1152. doi: 10.1002/hyp.10717

Zhou LT (2011) Impact of East Asian winter monsoon on rainfall over southeastern China and its dynamical process. Int J Climatol 31:677–686. doi:10.1002/joc.2101

Zhou B et al (2011) The great 2008 Chinese ice storm: its socioeconomic-ecological impact and sustainability lessons learned. Bull Am Meteorol Soc 92(1):47–60. doi: 10.1175/2010BAMS2857.1

Zhou T, Song F, Lin R, Chen X, Chen X (2013) The 2012 North China floods: explaining an extreme rainfall event in the context of along-term drying tendency [in"Explaining Extreme Events of 2012 from a Climate Perspective"]. Bull Am Meteorol Soc 94(9):S49-S51

Zhou B, Wen QH, Xu Y, Song L, Zhang X (2014) Projected changes in temperature and precipitation extremes in China by the CMIP5 multi-model ensembles. J Clim 27:6591–6611. doi: 10.1175/JCLI-D-13-00761.1

Zou L, Zhou T (2013) Near future (2016–2040) summer precipitation changes over China as projected by a regional climate model (RCM) under the RCP8.5 emissions scenario: comparison between RCM downscaling and the driving GCM. Adv Atmos Sci 30(3):806–818. doi:10.1007/s00376-013-2209-x

Zou L, Zhou T, Peng D (2016) Dynamical downscaling of historical climate over CORDEX East Asia domain: a comparison of regional ocean–atmosphere coupled model to stand-alone RCM simulations. J Geophys Res Atmos 121:1442–1458. doi:10.1002/2015JD023912